

Ultra High Speed Single-ended Traveling Wave Based Protection of Transmission Lines after Auto-reclosure

Mohammad Mohammadifirozjaee

A Thesis Submitted to
the Faculty of Graduate Studies
in Partial Fulfillment of the Requirements
for the Degree of
Master of Applied Science

Graduate Program in Electrical & Computer Engineering
York University
Toronto, Ontario

December 2018

© Mohammad Mohammadifirozjaee, 2018

Abstract

The auto-reclosure take place after a fault in power lines, in order to remove the temporary fault and reconnect the line as fast as possible. As there is no information whether the fault is temporary or permanent, the auto-reclosure will be carried out for permanent faults too. In the latter case, reconnecting the power line can result in extensive damage and it can even increase the restoration time. As a result, putting an end to auto-reclosure on a permanent fault is really important.

Considering the speed and reliability of the traveling wave protection method, this research considers it for an auto-reclosure case. Double-ended and single-ended traveling wave based protection schemes are proposed for after auto-reclosure using different parameters such as traveling waves attenuation, polarity and arrival time. Finally, extensive simulation has been carried out to verify the proposed scheme, where all the results confirm the effectiveness of the new practices.

Dedication

To my parents

Acknowledgments

I would like to express my gratitude to my supervisor Dr. Ali Hooshyar for kindly reading my reports and providing me with valuable comments.

I owe many thanks to my parents and my sister for their love, support and understanding through my study, who have been my source of inspiration and gave me strength.

Table of Contents

Abstract	ii
Dedication	iii
Acknowledgments	iv
Table of Contents	v
List of Tables	viii
List of Figures	ix
1 Introduction	1
1.1 Introduction to Power System Operation	1
1.2 Description of the Problem	2
1.3 Research Objectives	2
1.4 Dissertation Outline	3
2 Auto-reclosure	5
2.1 An Introduction on Auto-reclosure Process	5
2.2 Auto-reclosure History	7
2.3 Auto-reclosure Methods	7
2.3.1 High-speed vs. Low-speed	7
2.3.2 Multi-shot vs. Single-shot	8
2.3.3 Single-phase vs. Three-phase	9
2.4 Auto-reclosure Setting	9
2.4.1 Number of Auto-reclosures	10
2.4.2 Dead-time	10
2.4.3 Reclaim Time	13
2.5 Auto-reclosure Lockout/Blocking	14

2.6	Synchronism Check Relays	14
2.7	Conclusions	15
3	Traveling Waves	16
3.1	Introduction	16
3.2	The Theory Behind Traveling Waves	16
3.2.1	Transmission line equations	16
3.2.2	The Lossless Line	20
3.2.3	Propagation speed	22
3.3	Reflection and Refraction of Traveling Waves	22
3.4	Attenuation and Losses	24
3.5	Modal Transform	26
3.6	Traveling Wave Fault Location	26
3.6.1	Single-ended Method	26
3.6.2	Double-ended Method	27
3.7	Traveling wave fault protection	28
3.7.1	Single-ended Method	28
3.7.2	Double-ended Method	29
3.8	Summary	30
4	Traveling Waves Attenuation after Auto-reclosure	31
4.1	Proposed Solution	31
4.2	Performance Evaluation	40
4.2.1	Overhead line	40
4.2.2	Hybrid-line System	44
4.2.3	Effect of Fault Resistance	49
4.2.4	Effect of Fault Type	50
4.2.5	Effect of Fault Location	50
4.2.6	Effect of Line Length	52
4.2.7	Sensitivity of the Scheme to the Frequency	52
4.2.8	Attenuation in the Energy of the Traveling Waves	54
4.3	Conclusions	55
5	Single-ended Traveling Wave Based Protection after Auto-reclosure	56
5.1	Proposed Solutions	56
5.1.1	Polarity of Traveling Waves after Auto-reclosure	56
5.1.2	Arrival Time of Traveling Waves after Auto-reclosure	59
5.2	Simulation Results	59

5.2.1	Polarity of Traveling Waves after Auto-reclosure	60
5.2.2	Arrival Time of Traveling Waves after Auto-reclosure	64
5.3	Conclusions	68
6	Conclusions	69
6.1	Summary	69
6.2	Contributions	71
6.2.1	Analysis on the Attenuation of Traveling Waves	71
6.2.2	Single-ended Traveling Wave Based Protection after Auto-reclosure	72
6.3	Future Works	72
	Bibliography	73
	Appendices	76
A	PSCAD Customized Blocks for Traveling Waves	77
A.1	Traveling Wave First Zero Crossing Detection	77
A.2	Three Point Signal Average	78
A.3	Integrator	80
A.4	Clark Transform	80
A.5	Peak Locator	81
A.6	Traveling Waves Arrival Time Detection	82
A.7	Double-ended Traveling Wave Fault Location Relay	83

List of Tables

Table 1	MINIMUM DE-IONIZATION TIME REQUIRED FOR THREE PHASE FAULTS WITH RESPECT TO THE CIRCUIT VOLTAGE	12
Table 2	TRAVELING WAVE PROTECTION LOGIC USING TRAVELING WAVES POLARITY	30
Table 3	TRANSMISSION LINE ELECTRICAL PARAMETERS FOR OVER-HEAD LINE	41
Table 4	TRANSMISSION LINE ELECTRICAL PARAMETERS FOR HYBRID-LINE SYSTEM	46
Table 5	PROPOSED SCHEME UNDER DIFFERENT FAULT TYPES	51
Table 6	FAULT LOCATION EFFECT FOR DIFFERENT FAULT TYPES	53
Table 7	SENSITIVITY OF THE SCHEME TO THE FREQUENCY BY EMPLOYING ATTENUATION OF α COMPONENT	54
Table 8	ATTENUATION IN THE ENERGY OF THE TRAVELING WAVES	55
Table 9	TRANSMISSION LINE ELECTRICAL PARAMETERS	60
Table 10	POLARITY OF CURRENT TRAVELING WAVES AFTER AUTO-RECLOSURE ON CLOSED POWER LINE ($Z_L < Z_i$)	62
Table 11	POLARITY OF CURRENT TRAVELING WAVES AFTER AUTO-RECLOSURE ON OPEN POWER LINE ($Z_L > Z_i$)	63
Table 12	POLARITY OF VOLTAGE TRAVELING WAVES AFTER AUTO-RECLOSURE ON CLOSED POWER LINE ($Z_L < Z_i$)	64
Table 13	POLARITY OF CURRENT TRAVELING WAVES AFTER AUTO-RECLOSURE ON OPEN POWER LINE ($Z_L > Z_i$)	65

List of Figures

Figure 1	Single shot auto-reclosure operation scheme,(a) for temporary fault,(b) for permanent fault [1]	6
Figure 2	Equivalent model of segment of transmission line	17
Figure 3	Lattice diagram showing incident, reflected and transmitted traveling waves due to fault	23
Figure 4	Bewley lattice diagram after auto-reclosure on a permanent fault . . .	32
Figure 5	Traveling wave attenuation after successful auto-closure	33
Figure 6	Phase A to ground fault by resistance R	35
Figure 7	Traveling wave attenuation after auto-reclosure on permanent fault .	37
Figure 8	Proposed traveling wave based protection scheme for transmission lines after auto-reclosure	39
Figure 9	Traveling wave attenuation on hybrid line after successful auto-reclosure	39
Figure 10	Traveling wave attenuation on hybrid line with permanent fault . . .	40
Figure 11	The 230-kV overhead line model	41
Figure 12	Current traveling waves of aerial modes after successful auto-reclosure on overhead line, (a) Traveling wave captured at relay B, (b) Traveling wave captured at relay C	42
Figure 13	Current traveling waves of aerial modes for internal AG fault of overhead line, (a) Traveling wave captured at relay B, (b) Traveling wave captured at relay C	43
Figure 14	Current traveling waves of aerial modes for internal BC fault of overhead line, (a) Traveling wave captured at relay B, (b) Traveling wave captured at relay C	44
Figure 15	Current traveling waves of aerial modes for an external AG fault of overhead line, (a) Traveling wave captured at relay B, (b) Traveling wave captured at relay C	45
Figure 16	The 230-kV hybrid-line system model	45

Figure 17	Current traveling waves of aerial modes after successful auto-reclosure on hybrid-line system, (a) Traveling wave captured at relay B, (b) Traveling wave captured at relay C	47
Figure 18	Current traveling waves of aerial modes for internal AG fault of hybrid-line system, (a) Traveling wave captured at relay B, (b) Traveling wave captured at relay C	48
Figure 19	Current traveling waves of aerial modes for internal BC fault of hybrid-line system, (a) Traveling wave captured at relay B, (b) Traveling wave captured at relay C	48
Figure 20	Current traveling waves of aerial modes for external AG fault of hybrid-line system, (a) Traveling wave captured at relay B, (b) Traveling wave captured at relay C	49
Figure 21	Fault resistance effect for internal and external AG fault	50
Figure 22	Fault location effect for internal and external AG fault	52
Figure 23	Transmission line length effect for healthy line, internal and external AG fault	54
Figure 24	The 230-kV overhead line model	60
Figure 25	Current traveling waves of aerial modes after unsuccessful auto-reclosure for AG fault on overhead line	66
Figure 26	Current traveling waves of aerial modes after successful auto-reclosure for AG fault on overhead line	66
Figure 27	Current traveling waves of aerial modes after unsuccessful auto-reclosure for BG fault on overhead line	67
Figure 28	Current traveling waves of aerial modes after successful auto-reclosure for BG fault on overhead line	67
Figure 29	Customized traveling wave first zero cross detection block for PSCAD	77
Figure 30	Customized three point signal average block for PSCAD	78
Figure 31	Customized integrator block	80
Figure 32	Clark transform block for PSCAD	81
Figure 33	Traveling wave first peak detection	81
Figure 34	Traveling waves arrival time block for PSCAD	82
Figure 35	Double-ended traveling wave fault location relay designed in PSCAD	83
Figure 36	Defined parameters for double-ended traveling wave fault location relay	84

Chapter 1

Introduction

1.1 Introduction to Power System Operation

The electric power grid has played a major role in the technological advancements of the recent decades. Power grid is defined as a network of transmission lines connecting power generation stations to the customers. Power lines are inevitable parts of power systems which their performance and efficiency have a significant effect on the way electricity is generated and transmitted. Particularly, in cases where there is a long distance between the power plant and customers, their protection require higher attention as there is a higher chance of failure.

One of the most serious problems in transmission lines is the occurrence of fault which largely affect the quality of the supplied power. These faults are categorized into temporary, semi-transient and permanent. The temporary fault can be a result of lightning and is removed over time owing to its transient nature. The semi-permanent faults are removed following the re-energization of the transmission line, for instance a branch of tree which falls on the line and burns during re-energization. The permanent fault cannot be removed and the transmission line has to be repaired before reconnecting it. Whatever the kind of fault is, the power line has to be disconnected through the use of fault protection devices as quickly as possible. These fault protection devices work via different fault protection approaches, which have been the subject of so much research with the objective of improving their speed and security. As faster protection system means a higher reliability, resulting in higher power transmission and subsequently higher efficiency.

1.2 Description of the Problem

From the earliest days of electric power grid, engineers have endeavored to ameliorate power system protection by enhancing its security, dependability, speed, and sensitivity. However, with the advent of Extra High Voltage (EHV) lines, the speed has been given a much higher importance as a fast removal of faults is the best measure to improve power-line capacity and system stability. As a result, high speed protection of power line at any condition is a necessity, where one of these conditions is the auto-reclosure.

The auto-reclosure scheme is applied to remove the fault on a power line; provided the fault is temporary, the auto-reclosure will be successful in minimizing the outage time as a result of the fault. However, no information regarding the fault status is obtained until the reconnection process begins. After reconnecting the line, there are two possibilities; first, the fault is temporary and will pass; second the fault is permanent which means the auto-reclosure was unsuccessful and the line has to be disconnected by a protection device. Formal protection methods such as over-current relay can detect the fault following auto-reclosure; such methods, on the other hand, are slow and cannot compete with the protection needs of new power systems, hence the necessity of a high-speed protection after auto-reclosure.

The latest and fastest protection method is the traveling wave method, which has not been accommodated for protection after auto-reclosure. All traveling wave protection methods rely on traveling waves generated by fault abnormal currents; however, after auto-reclosure, traveling waves are generated by breaker operation rather than the fault. Due to breaker operation, traveling waves do not carry any information regarding the fault. As a result, different methods and procedures are needed to capture and analyze the traveling waves after auto-reclosure so as to protect the power line.

1.3 Research Objectives

Protection challenges after auto-reclosure could be tackled via two different approaches of traveling wave protection:

1. Recognizing the fault after auto-reclosure using the traveling waves captured at local and remote terminals.
2. Finding out the transmission line status after auto-reclosure by use of successive traveling waves captured at the local terminals.

The first approach requires two relays at the local and remote terminals and a communication channel. The research on the first method is focused on using the arrival time of traveling waves to find the right traveling wave and using the attenuation to address the problem. The attenuation of the traveling wave has not been used for protection application yet, as a result, a theoretical background will be provided. Moreover, the research will focus on providing an ultra high-speed algorithm which is super-fast and reliable at the same time.

The second method does not need any communication channel, hence it is cheaper. But, it is harder to devise protection schemes as there is information merely on the successive traveling waves captured at the local terminal. To address this issue, well-known traveling wave protection methods such as polarity and arrival time are utilized. Different simulation studies have managed to examine each of these parameters and theoretical and physical explanations have been provided. The final result of this section proposes a fast, secure and reliable traveling wave-based logic to protect power line following auto-reclosure.

As a protection study, this research has been driven to answer the protection need after auto-reclosure using the available industrial relays, one of which is SEL 401 which captures traveling waves and use them for protection needs during normal operation of the power line. The proposed protection methods can be added in these relays as new protection elements, as all the data required for this traveling wave method is available.

On this basis, the thesis was driven by the objective of providing fast protection after auto-reclosure using the available traveling wave relay. The following constraints were considered on the way of meeting the objectives.

1. No extra hardware was needed other than the currently available ones.
2. The solution must not need any new traveling wave capturing algorithm.

1.4 Dissertation Outline

This thesis is divided into two main parts. The first three chapters provide information on tackling the problem of high-speed auto-reclosure and the subsequent two, explain the proposed solutions and simulation results. Each individual chapter is organized as follows:

- Chapter 2 elaborates on the performance and application of auto-reclosure practice in power systems. It commences with an introduction on auto-reclosure following a description on its methods. The comparison takes place among methods based on their

speed, and number of operations and procedure, which can be single phase or three phase, and single-shot or multi-shot. In the end, different parameters influencing auto-reclosure are explained as the required settings of auto-reclosure.

- Chapter 3 begins with an introduction on traveling waves, their history and theoretical background. The drawbacks and benefits of both double-ended and single-ended traveling wave methods are further elucidated. Moreover, the application of traveling waves for fault location is put forth and explained for the two available methods, the double-ended and single-ended.
- Chapter 4 states the problem encountered by the traveling wave-based protection after auto-reclosure and provides solution based on traveling wave arrival time and attenuation. The section focuses on the effects of traveling wave attenuation by fault resistance and transmission line impedance. Next, the proposed algorithm, which uses a combination of traveling wave attenuations and arrival times, is explained. The simulation model is further proposed and elucidated in details. Finally, the performance of the traveling wave-based protection is evaluated by an extensive simulation.
- Chapter 5 concentrates on addressing traveling wave based after auto-reclosure protection using successive traveling wave captured at local terminal. The proposed solution is explained based on polarity and arrival time of traveling waves, and the proposed methods are ultimately put through extensive simulation. The last section proposes the combination of all parameters to increase the security and reliability of this method.
- Chapter 6 concludes the whole dissertation: First, it provides a summary of the proposed methods and simulation results. The contribution of this thesis to the industry and academia is also explained. Finally, the future work section elaborates possible strategies to ameliorate the proposed protection methods.

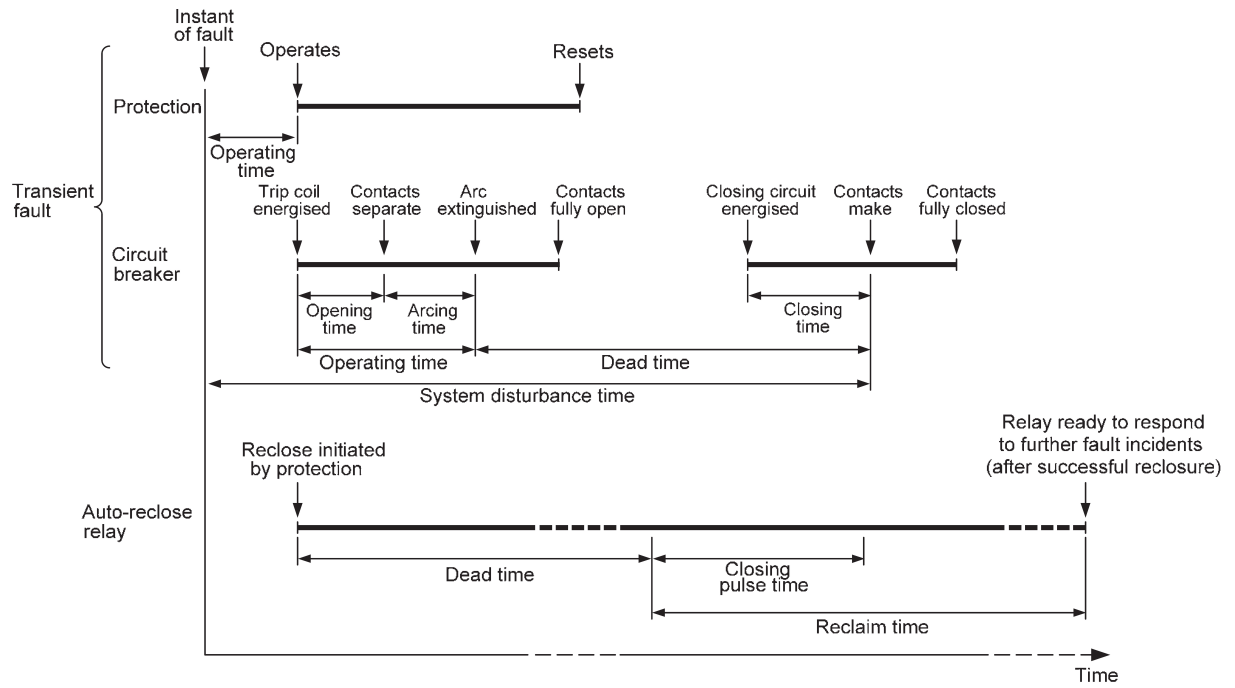
Chapter 2

Auto-reclosure

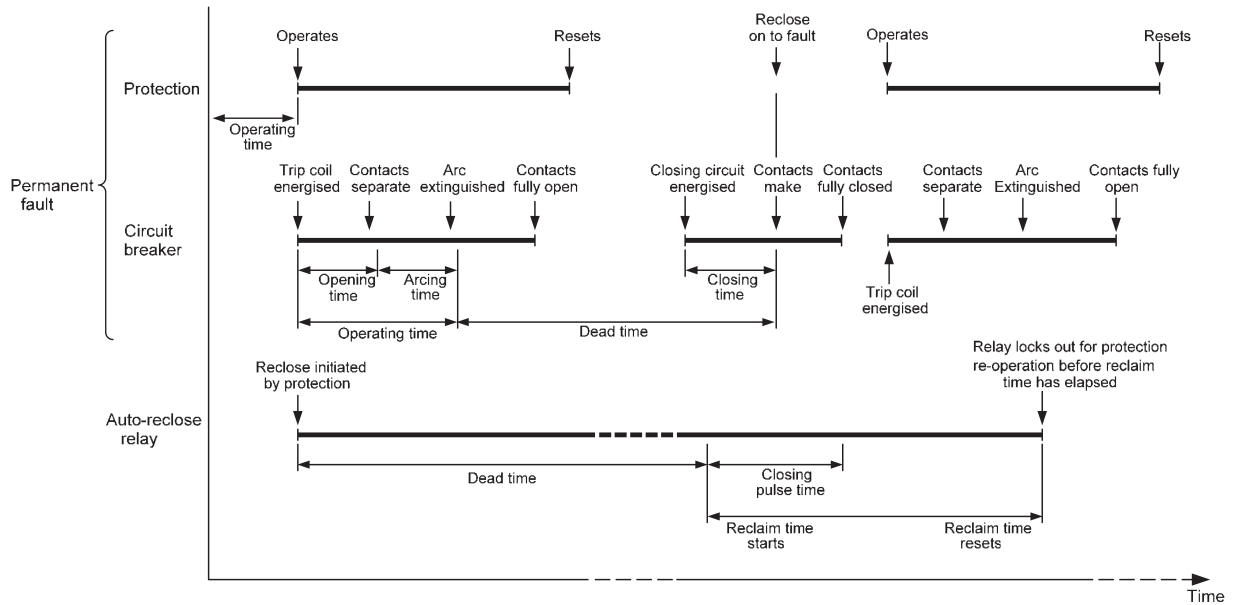
2.1 An Introduction on Auto-reclosure Process

Auto re-closure is a common practice, in power systems, which consists of breaking and reconnecting the transmission line in order to remove the temporary faults and reconnect the power line as fast as possible. In order to reach a successful auto-reclosure and eliminating the temporary faults, transmission line should be completely de-energized first, and then it should be reconnected after a specific amount of time which is called dead time. The dead time can be low or high depending on the requirement of power system. The most important criteria to choose between high and low-speed auto-reclosure is the dead time, which is affected by the loading type, system stability and synchronization needs and circuit breaker characteristics. The auto-reclosure scheme can be single-shot or multi-shot which means the auto-reclosure can be done just once or multiple times to reach a successful re-energization. Figure 1 provides successful and unsuccessful single-shot auto-reclosure scheme, where the reclaimed time is the time between reconnecting the transmission line and reaching the steady state condition of a power system. The most important parameters of an auto-reclosure scheme are dead time, reclaim time and number of auto-reclosure attempts where choosing them is mostly dependent on statistical analysis.

Auto-reclosure often takes place for power lines with the overhead lines, as faults in underground cables are regularly permanent and the re-energization can result in extensive damage. However, in case of hybrid lines where the power line is mostly consisted of overhead transmission line and some part of underground cables, the auto-reclosure is still logical, as there is a high possibility for temporary faults in overhead power lines. However, due to system sensitivity, only single-shot scheme is considered. This kind of



(a)



(b)

Figure 1: Single shot auto-reclosure operation scheme,(a) for temporary fault,(b) for permanent fault [1]

power line is really probable as the use of overhead lines over a river and some urban areas are prohibited and the underground tunnels are used to transmit power for short distances due to its higher cost.

2.2 Auto-reclosure History

The auto-reclosure procedure was first employed in 20's century. Further studies indicated that it is successful in more than 70 percent of cases [2]. As a result, currently it has been utilized for most of the power transmission lines.

To provide more efficient auto-reclosure, the Single-Phase Auto-Reclosure (*SPAR*) was proposed to enhance the stability of power system. Different parameters were employed for SPAR such as the value of the induced voltage on faulty lines or the root mean square (*RMS*) value of faulted phase voltage [3, 4]. Other works in this area considered using Artificial Intelligence (*AI*) methodology too.

All these achievements are the result of improvements in circuit breaker design and mechanism, which decreased their operation time. It should be noted that more than improvement in circuit breaker, the enhancements in solid state technology and digital electronic paved the way for the new approaches too.

2.3 Auto-reclosure Methods

Auto-reclosure can be carried out by different schemes, but there are three general parameters that can specify auto-reclosure. The speed, number of shots and number of phases which auto-reclosure will be carried out on. A brief comparison of each method will be provided in the next sections.

2.3.1 High-speed vs. Low-speed

In case the dead time is sufficiently low the auto-reclosure scheme will be called high speed. In the mentioned scheme, the power line will be reconnected faster and outage time will be lower; however, there will be a higher chance of unsuccessful auto-reclosure, as some of the temporary and semi transient faults require higher dead time in order of removal. However, it's more favorable as the outage time will be reduced. It's mostly implemented

on a power line where the fast reconnection is more important than damages on power line appliances. To employ high-speed auto-reclosure, power system equipment should pose some features such as:

- System should be strong enough to hold the phase angle differences until auto-reclosure is carried out
- High-speed protection should be employed on all terminals
- Voltage induction from parallel line, should not sustain fault after auto-reclosure

There are some factors which affect high speed auto-reclosure success, including:

- Fault clearance time
- Fault current magnitude
- Weather condition
- Transmission line location
- Instantaneous voltage value during line re-energization

In low-speed auto-reclosure, the dead time is more and there is a higher chance of successful auto-reclosure. In some power lines where there is back up line or parallel line, the low speed or delayed auto-reclosure is more applicable, as there is no necessity for fast auto-reclosure. The time delay which added to the arc de-ionization time in order to reach low-speed auto-reclosure is mostly between 1 to 60 seconds based on the systems condition [5]. It should be noted that in most cases due to the costs of building parallel lines, there is no back up power line, or as the backup lines don't have enough capacity, the high-speed protection is a priority.

2.3.2 Multi-shot vs. Single-shot

There is no definite number of shots for auto-reclosure; however, there is a number of factors which can affect it. The first definite one is the power system condition, which can be obtained from statistical reviews. If a power system shows a moderate percentage of

semi-permanent fault which could be removed by two or three trip actions; then, the multi-shot schemes would be justified. However, in case of sensitive systems such as *EHV* lines, unsuccessful attempts can result in disastrous damages to the system or even high-level fault can lead to a bush-fire, where the multi-shot procedure could not be carried out. The other limitation is circuit breakers ability to performs multiple trip actions. Moreover, the maintenance period of circuit breakers should be taken into account, as the circuit breaker may not be able to perform successive trips after it passes the required maintenance period.

2.3.3 Single-phase vs. Three-phase

In single-phase auto-reclosure, the auto-reclosure procedure will be only carried out on one phase. The benefit of this method originates from the remaining healthy phases that can transfer some part of the pre-fault power. Considering the fact that more than 90% of faults on transmission lines are a single phase to ground, the single pole auto-reclosure will be more suitable to meet the needs of new power lines as means of improving transient stability and reliability [6]. However, there are problems with *SPAR*, the major one is the affection of ground protection as a result of ground current circulation. Also, each pole should be equipped with an independent tripping mechanism. Generally speaking, the advantage of *SPAR* versus the three-phase auto-reclosure is the maintenance of system integrity and also negligible interference with the transmitted power through the line.

In comparison, the three-phase auto-reclosure will trip all phases and perform auto-reclosure on all three phases at the same time without considering which phase was faulty. Generally, three phase auto-reclosure may take place if the *SPAR* fails, the multi-phase fault was recognized or more phases become involved in fault after the single-phase tripping.

2.4 Auto-reclosure Setting

There are different parameters for auto-reclosure setting such as:

- Number of auto-reclosures
- Dead-time
- Auto-reclosure reset-time

These parameters will be effected by:

- Type of protection
- Type of switchgear
- Possible stability problems
- The effects on consumers

The given importance to each of parameters above will depend on the type of power system which could be *EHV* transmission line or *HV* distribution networks. Different control schemes were developed based on these parameters which will be discussed in the following sections in detail.

2.4.1 Number of Auto-reclosures

As discussed earlier, auto-reclosure can be single-shot which means it will perform only once, or it can be multi-shot where auto-reclosure will be attempted several times. The single-shot auto-reclosure is the simplest choice; however, the disadvantage of any outage on power systems, force engineers to accept the risks of multiple auto-reclosure in order to reconnect the line as fast as possible.

In *HV* distribution networks, multi-shot reclosing is common. However, the multi-shot scheme should be designed based on circuit breaker limitation and system condition. Circuit breakers limitation is the available gas or air pressure, and the maintenance periods. The ability of circuit breaker to perform a quick multiple trip and close, will be reduced over time based on the amount of each fault current. Modern numerical relays help to estimate the maintenance period and to lock out the breaker if it is passed. Regarding the system condition, in case the statistical reports indicate a high number of temporary faults that could be burned, the multi-shot scheme will make sense. However, the fault current and fuse limitation should be considered as well, as too many reclosing on permanent fault will heat the fuse and may blow it before the main protection act.

In *EHV* systems, the multi-shot auto-reclosure is not applicable, due to the system sensibility; and the circuit breaker will be locked out after the first unsuccessful auto-reclosure.

2.4.2 Dead-time

Before conducting the auto-reclosure procedure, it should be noted that although fast reconnection of the transmission line is important, but reclosing without proper time delay

will result in failed auto-reclosure. The reason is that if the time delay is not enough, the arc may not extinguish by the time the reclosing take place. The de-ionization time for arc depends on various factors such as weather condition, voltage, fault current and conductors spacing. For example, the minimum dead time can be found in the simplest way using the following formula:

$$t = 10.5 + \frac{V_{L-L}}{34.5} \quad (2.1)$$

where t is considered as the time delay in power cycles and V_{L-L} is the line rated voltage in KV [5]. The exact amount of dead time will be determined by thoroughly considering various factors such as:

- Fault de-ionization time
- Type of load
- Circuit breaker characteristics
- System stability and synchronization
- Protection reset time

Each of these factors are discussed in the following sections in order to give more insight into their required setting.

Fault de-ionization time

As mentioned previously, the dead time should be sufficient to de-ionize fault arc. If the dead time is not long enough, the ionized air will result in another arc. This time is based on system voltage, weather condition, and fault cause. On systems with the voltage up to $66KV$, statistics prove that the de-ionization time of 0.1 to $0.2sec.$ should be enough. Among the parameters effecting fault de-ionization time, circuit voltage is the most important one, where a higher voltage results in longer de-ionization time. Table 1 provides the minimum dead time required for de-ionization of three-phase fault for different circuit voltages.

TABLE 1:
MINIMUM DE-IONIZATION TIME REQUIRED FOR THREE PHASE FAULTS
WITH RESPECT TO THE CIRCUIT VOLTAGE

Line Voltage (kV)	Minimum De-energisation Time (sec.)
66	0.2
110	0.28
132	0.3
220	0.35
275	0.38
400	0.45
525	0.55

Loading type

The main factor to choose dead time in *HV* lines is the loading type. Generally, loads can be specified as industrial or domestic consumers.

For industrial consumers, there is a mixed load which mostly includes the induction motors and lightening. The most important thing is that the dead time should be long enough to allow electrical motors to trip out. Then, reclosing can proceed by the control process and usually it will be fast enough not to make any significant damages to the production lines.

For domestic users longer dead time is more applicable as a dead time of even a few seconds is not comparable to the loss of power for hours. Generally, domestic users can take higher blackouts as there is no dangerous or expensive process, and power loss can be compensated after auto-reclosure.

Circuit breaker characteristics

Circuit breaker will affect dead time because of its limitation from mechanical constraints. The time delay can be expressed as a mechanical reset and closing time as it follows.

Mechanism reset time will be affected by operation speed of circuit breaker. Currently, most of the circuit breakers are able to trip off even at the time of closing stroke. However, after each trip, the time delay of approximately 0.2sec. should be considered for mechanism reset time.

The closing time of the breaker will depend on the type of circuit breaker being used. This time starts from the moment that reclosing signal is transmitted until the contacts are made. A solenoid mechanism may take up to $0.3sec.$ to close; whereas the spring operated one takes less than $0.2sec.$ However, modern circuit breakers which work in a vacuum can reclose even in less than $0.1sec.$

Finally, the minimum dead time needed due to circuit breakers constraints will be the sum of resetting and closing time.

System stability and synchronization

The most important part of auto-reclosure is about maintaining the system stability and synchronization and if they have not been met, the auto-reclosure will be useless. To maintain the system stability, the dead time should be short enough and time delay should be kept as limited as possible. The problems arising from system stability and synchronization can be considered for two different types of systems, the weak and the strong systems. In weak systems, the phase angle will change really fast after tripping the line. As a result, high-speed auto-reclosure should be carried out to prevent unsuccessful auto-reclosure. However, in strong systems the rate of change in phase angle after tripping will be slow; consequently, the time delayed auto-reclosure can be put in practice.

Protection reset time

In case of time-delayed auto-reclosure, the dead time should be sufficient for relay timing devices to reset before reclosing. It's necessary to maintain the correct time discrimination after auto-reclosure on the power line with a fault. The time needed for an electromechanical relay to reset is at least $10sec.$, which is not proper for high-speed auto-reclosure. However, numerical and digital relays can reset instantly which make them proper for high-speed auto-reclosure or lower time delayed auto-reclosure cases.

2.4.3 Reclaim Time

After auto-reclosure, power line protection devices should reset to become ready for any future faults. This could be done by reset timer and the time after dead-time until protection devices reset will be considered as reclaim time. Choosing relay reset time delay is affected by nature of fault and its clearance time. For instance, the chance of unsuccessful auto-reclosure and re-tripping will increase with lower reset time delay.

2.5 Auto-reclosure Lockout/Blocking

If auto-reclosure is unsuccessful for multiple times and it exceeds the predetermined number of attempts, automatic reclosing will be locked. More than system stability reasons, stopping multiple unsuccessful auto-reclosure prevent too many wears from the relay and decrease its maintenance costs. Generally, auto-reclosure will be blocked in different cases such as:

- 1) Supervisory monitoring voltage: If relay monitors any voltage on power line it will block auto-reclosure. This kind of supervision is commonly employed for power lines with solid sources such as large generators or motors to avoid any kind of damages to rotary devices.
- 2) Operator tripping: If a circuit breaker trips manually or by the remote control signal, auto-reclosure will be blocked as the preferences will be given to the operator for reclosing.
- 3) Fault in underground cables, bus or transformer: These kind of faults are permanent in nature and reclosing the line after tripping will aggravate the damage and increase the time needed for repairing the line.
- 4) Circuit breaker failure: Auto-reclosure will be blocked in the case of the circuit breaker failure, to isolate the failed circuit breaker and bus restoration.
- 5) Circuit breaker reclosing failure: If circuit breaker reclosing attempt fails or it takes longer than the expected time, auto-reclosure scheme will be blocked in order to stop any further damages to the power line.

2.6 Synchronism Check Relays

Synchronism check relay is employed to make sure that system stability and synchronization will maintain after auto-reclosure. Synchronism check relay uses two main factors to determine system synchronization:

- Phase angle difference
- Voltage

Relay permits auto-reclosure only when phase angle difference is between 20° to 45° . If it exceeds this amount, relay stops reclosing until this criteria is met. However, if auto-reclosure does not perform after 5 sec., most relay will lock out reclosing scheme.

Measured voltage is another criterion, where synchronism check relay is looking for under voltage in either of the two measured voltages, in differential voltage or both of them.

2.7 Conclusions

The presented chapter provided an introduction to auto-reclosure schemes, its benefits and characteristics. As discussed earlier, both breakers from the local and remote terminal should be tripped, in order to provide the dead-time and fault arc de-ionization. Following the dead-time, it's a common procedure to first reclose one of the breakers to energize the line. Then, the synchronism check relay will permit the second breaker reclosing. In case of a permanent fault, the whole process will repeat if the system is strong enough and circuit breakers have the ability to reclose again. But if the fault is temporary, it will probably extinguish and the power line will return to its normal condition. After each auto-reclosure, protection devices should be ready to trip the line, as the fault may still exist. To reduce the negative effects of reclosing on permanent faults to power system stability and maintenance, high-speed protection should be used to trip the power line as fast as possible. One of the newest and fastest existing methods is the traveling wave method which is gradually replacing the older protection methods. However, there is no traveling wave scheme proposed for after auto-reclosure protection. Therefore, due to the salient features of high-speed protection after auto-reclosure, this dissertation will propose different traveling wave scheme to carry out power line protection after auto-reclosure.

Chapter 3

Traveling Waves

3.1 Introduction

Traveling waves are high-frequency transients of power system. Traveling waves occur by any sudden changes in a power line. These irregularities may include switching, lightning, or the faults attributed to insulation failures but they are not limited to these features. Current or voltage traveling waves could be typically revealed on power lines which operate by $50Hz$ and are more than $80km$ [7].

3.2 The Theory Behind Traveling Waves

The resistance and inductances of transmission line conductors are consistently distributed along the line. These parameters can be demonstrated in equivalent series of PI circuits. Applying such a modeling is crucial for the analysis of power line and traveling waves. Therefore, in the following sections, the mentioned modeling is applied in order to define a transmission line equation and extract traveling waves.

3.2.1 Transmission line equations

As mentioned earlier, any change in the steady state condition of power quantities which can be any disturbance at any point on the transmission line, will result in the traveling waves. It is important to mention that the traveling wave is just for circuits with lumpiness

characteristics. Lumpiness comes from the response of transmission line components such as a reactor and capacitors, to a stimulus. Consequently, there is no traveling wave in simple lines with just a resistance. To investigate the equation and study the behavior of these traveling waves, it is important to consider a small section of transmission line length including the equivalent electrical parameters as demonstrated in Figure 2.

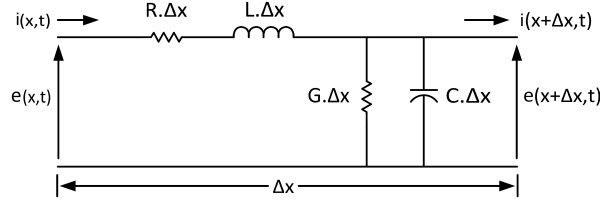


Figure 2: Equivalent model of segment of transmission line

where Δx is the line segment with resistance (R), conductance (G), capacitance (C), and inductance (L), all in per unit length. By calculating the voltage drop through the distance of Δx of the transmission line the following reveals:

$$e(x, t) - e(x + \Delta(x), t) = R\Delta(x)i(x, t) + L\Delta(x)\frac{\delta(i(x, t))}{\delta(t)} \quad (3.1)$$

Applying Kirchhoffs current law for a current flow through conductance (G) and capacitance (C) result in:

$$i(x, t) - i(x + \Delta(x), t) = G\Delta(x)e(x + \Delta(x), t) + C\Delta(x)\frac{\delta(e(x + \Delta(x), t))}{\delta(t)} \quad (3.2)$$

Considering Δx approaches zero, the derivative of current and voltage with considering the position (x) could be obtained. Therefore, a cancellation in changing the positions of (3.1) and (3.2) will result in:

$$\frac{\delta e(x, t)}{\delta x} = -Ri(x, t) - L\frac{\delta i(x, t)}{\delta t} \quad (3.3)$$

and,

$$\frac{\delta i(x, t)}{\delta x} = -Ge(x, t) - C\frac{\delta e(x, t)}{\delta t} \quad (3.4)$$

Substituting the Heaviside operator:

$$s = \frac{\delta}{\delta t} \quad (3.5)$$

and using $Z = R + Ls$ and $Y = G + Cs$ the following equations could be obtained by considering the above mentioned facts:

$$\frac{\delta e(x, s)}{\delta x} = -Zi(x, s) \quad (3.6)$$

$$\frac{\delta i(x, s)}{\delta x} = -Ye(x, s) \quad (3.7)$$

Through the differentiation by x for one more time, it is more probable to achieve the goal of separating voltage and current equations.

$$\frac{\delta^2 e(x, s)}{\delta x^2} = -Z \frac{\delta i(x, s)}{\delta x} \quad (3.8)$$

$$\frac{\delta^2 i(x, s)}{\delta x^2} = -Y \frac{\delta e(x, s)}{\delta x} \quad (3.9)$$

The substitution of (3.6) and (3.7) in (3.8) and (3.9), result in the second partial differential equation as follows:

$$\frac{\delta^2 e(x, s)}{\delta x^2} = ZY e(x, s) \quad (3.10)$$

$$\frac{\delta^2 i(x, s)}{\delta x^2} = YZ i(x, s) \quad (3.11)$$

where the square root of ZY for the transmission line is equal to the propagation constant γ of traveling waves, which provide their amplitude and phase variation along the transmission line. Bear it in mind, (3.10) and (3.11) can be written as:

$$\frac{\delta^2 e(x, s)}{\delta x^2} = \gamma^2 e(x, s) \quad (3.12)$$

$$\frac{\delta^2 i(x, s)}{\delta x^2} = \gamma^2 i(x, s) \quad (3.13)$$

The general solution to these equations is detailed below:

$$e(x, t) = e_I \exp^{-\gamma x} + e_R \exp^{\gamma x} \quad (3.14)$$

$$i(x, t) = i_I \exp^{-\gamma x} + i_R \exp^{\gamma x} \quad (3.15)$$

where, $e_I \exp^{-\gamma x}$ and $i_I \exp^{-\gamma x}$ are referring to the incident wave and $e_R \exp^{\gamma x}$, $i_R \exp^{\gamma x}$ are referring to the reflected waves of current and voltage. The ratio between current and voltage of incident and the reflected components define the characteristic impedance of transmission line which can be written for the incident and reflected wave as:

$$Z_C = \frac{e_I}{i_I} = \sqrt{\frac{Z}{Y}} \quad (3.16)$$

$$Z_C = -\frac{e_R}{i_R} = \sqrt{\frac{Z}{Y}} \quad (3.17)$$

which can also be written as follow:

$$Z_C = \sqrt{\frac{R + L \frac{\delta}{\delta t}}{G + C \frac{\delta}{\delta t}}} \quad (3.18)$$

Finally, (3.15) can be written with voltage parameters as:

$$i(x, t) = \frac{1}{Z_C} (e_I \exp^{-\gamma x} - e_R \exp^{\gamma x}) \quad (3.19)$$

Solving these equations will be different for each disturbance case and a set of boundary conditions which will be discussed in detail in the following sections.

3.2.2 The Lossless Line

Solving the equation by considering lossless line, where resistance and conductance are equal to zero will be easier and it will facilitate the perception of traveling wave propagation as well. In this case, the transmission line equations will become as follow:

$$\frac{\delta e}{\delta x} = -L \frac{\delta i}{\delta t} \quad (3.20)$$

and,

$$\frac{\delta i}{\delta x} = -C \frac{\delta e}{\delta t} \quad (3.21)$$

Since the resistance and conductance are zero, there will be no damping and steady wave solution can be defined as:

$$e = Z_C i \quad (3.22)$$

In case of using (3.22), (3.20) and (3.21) can be written as:

$$Z_C \frac{\delta i}{\delta x} = -L \frac{\delta i}{\delta t} \quad (3.23)$$

and,

$$\frac{\delta i}{\delta x} = -Z_C C \frac{\delta i}{\delta t} \quad (3.24)$$

Dividing these two equations, Z_C could be obtained as:

$$Z_C = \sqrt{\frac{L}{C}} \quad (3.25)$$

which will be equal to the characteristic impedance of the lossless line. The partial equation for the lossless line will be equal to:

$$\frac{\delta^2 e}{\delta x^2} = LC e \quad (3.26)$$

which implies that the traveling waves shapes do not change by traveling on the lossless transmission line [8]. In this case, the general solution for current and voltage traveling waves will be shortened to:

$$e(x, t) = e_I \exp^{\frac{x}{v}} + e_R \exp^{-\frac{x}{v}} \quad (3.27)$$

and,

$$i(x, t) = -\frac{1}{Z_C} (e_I \exp^{\frac{x}{v}} - e_R \exp^{-\frac{x}{v}}) \quad (3.28)$$

where v is indicating the propagation speed of traveling wave equal to:

$$v = \frac{1}{\sqrt{LC}} \quad (3.29)$$

At the present step, Taylor's series can be applied to approximate this function with a series in order to simplify it.

$$A(t + h) = A(t) + hA'(t) + (\frac{h^2}{2!})A'' + \dots = (1 + hs + \frac{h^2}{2}s^2 + \dots)A(t) = e^{hs} A(t) \quad (3.30)$$

Applying Taylor's series to (3.27) and (3.28) will result in the following solution for current and voltage traveling waves in the time domain as:

$$e(x, t) = e_I(t + \frac{x}{v}) + e_R(t - \frac{x}{v}) \quad (3.31)$$

$$i(x, t) = -\frac{1}{Z_C} (e_I(t + \frac{x}{v}) - e_R(t - \frac{x}{v})) \quad (3.32)$$

where expression $e_I(t + \frac{x}{v})$ is the description of wave propagation in the negative direction called backward wave, and $e_R(t - \frac{x}{v})$ is an explanation of wave propagation in positive direction of x [9].

3.2.3 Propagation speed

Both forward and backward traveling waves propagate with a velocity v which is close to the light speed, i.e. $3 \times 10^8 m/s$; however, finding the exact amount is necessary for traveling waves applications. From the voltage drop equation in lossless line:

$$e(x, t) - e(x + dx, t) = (Ldx) \frac{\delta i(x, t)}{\delta t} \quad (3.33)$$

and as $e = Z_C i$, (3.33) can be written as:

$$i(x, t) - i(x + dx, t) = \left(\frac{L}{Z_C} dx\right) \frac{\delta i(x, t)}{\delta t} \quad (3.34)$$

where $\frac{\delta i(x, t)}{\delta t}$ is considered as finite, following can be obtained from (3.34).

$$i(x, t) - i(x + dx, t) = \left(\frac{L}{Z_C} dx\right) \frac{i(x, t) - i(x + dx, t)}{dt} \quad (3.35)$$

Finally, $\frac{dx}{dt}$ which is equal to wave propagation speed, can be found as:

$$v = \frac{dx}{dt} = \frac{Z_C}{L} e = \frac{1}{\sqrt{LC}} \quad (3.36)$$

3.3 Reflection and Refraction of Traveling Waves

Assuming fault taking place on power line illustrated in Figure 3, there will be traveling waves toward local terminal (L) and remote terminal (R). t_{L1} and t_{R1} are the arrival time of traveling waves at local and remote terminal. Traveling waves will move to the two ends of the line without any specific changes unless it encounters discontinuity. At each discontinuity which can be for example a bus or fault, a part of the traveling wave transmitted and the remaining will be reflected. This phenomenon is perfectly indicated in Bewleys Lattice diagram provided in Figure 3.

At each discontinuity, the incident wave energy will be divided between the reflected and transmitted waves. The reflection and transmission process last until the incident traveling wave damp and lose its energy. To find the amplitude of transmitted and reflected traveling waves, characteristic impedance Z_C is a key parameter. Z_C can be found as:

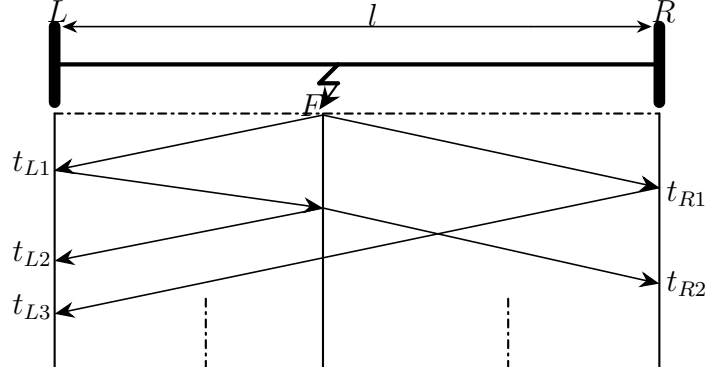


Figure 3: Lattice diagram showing incident, reflected and transmitted traveling waves due to fault

$$Z_C = \frac{e_i}{i_i} = -\frac{e_r}{i_r} \quad (3.37)$$

where, e_i , i_i indicating the voltage and current traveling waves in forward direction or the incident wave and e_r , i_r indicating the voltage and current traveling waves propagating in negative direction which is the reflected traveling wave. Considering e_t and i_t as the voltage and current of the transmitted traveling wave, the impedance seen by the transmitted traveling wave Z_t can be written as:

$$Z_t = \frac{e_t}{i_t} \quad (3.38)$$

As the current and voltage traveling waves are obviously continuous at junction point, the voltage and current can be described based on boundary condition as:

$$e_t = e_i + e_r \quad (3.39)$$

and,

$$i_t = i_i + i_r \quad (3.40)$$

where using (3.39) and (3.40), Z_t reveal as:

$$Z_t = \frac{e_i + e_r}{i_i + i_r} \quad (3.41)$$

The substitution of i_i and i_r from equations at (3.37) to acquire voltages will result in:

$$\frac{Z_t}{Z_C} = \frac{e_i + e_r}{e_i - e_r} \quad (3.42)$$

Rearranging this equation provide the ratio, called the voltage reflection factor ρ_e given by:

$$\rho_e = \frac{e_r}{e_i} = \frac{Z_t - Z_C}{Z_t + Z_C} \quad (3.43)$$

and similarly, for the current traveling wave reflection ratio ρ_i can be written as:

$$\rho_i = \frac{i_r}{i_i} = \frac{Z_C - Z_t}{Z_C + Z_t} \quad (3.44)$$

3.4 Attenuation and Losses

Traveling waves attenuate and disperse during their travel through the transmission line due to the transmission line resistance and conductance. In order to analyze the traveling waves propagation through the transmission line with multiple conductors, the modal analysis should be employed to decouple the traveling waves modes. To decouple the wave propagation in three phases, the propagation matrices of A_e and A_i should be considered as follows.

$$A_e = ZY \quad (3.45)$$

$$A_i = YZ \quad (3.46)$$

where Z and Y are the impedance and admittance matrices of the transmission line. Next, the ideal matrix of T_i and T_e should be created to set up the diagonal matrix of Λ as detailed below:

$$\Lambda = T_e^{-1} A_e T_e \quad (3.47)$$

$$\Lambda = T_i^{-1} A_i T_i \quad (3.48)$$

$$\Lambda = \begin{bmatrix} \lambda_1 & \dots & 0 \\ \vdots & \ddots & \vdots \\ 0 & \dots & \lambda_m \end{bmatrix} \quad (3.49)$$

where the square root of each Eigen values (λ_m) in Λ , represents the wave propagation constant (γ_m) by the following equation:

$$\gamma_m = \sqrt{\lambda_m} \quad (3.50)$$

Finally, the attenuation for each mode (α_m) can be found from the real part of γ_m , and the imaginary part (β_m) provides the phase constant.

$$\gamma_m = \alpha_m + j\beta_m \quad (3.51)$$

The non-zero value for (α_m) indicates that there are line resistances and conductance which result in wave attenuation and damping. However, the imaginary part β_m indicate that the propagation velocity of the traveling wave depends on frequency, which can be written as:

$$v_m = \frac{w}{\beta_m} \quad (3.52)$$

The propagation velocity depends on frequency and could be viewed from a different perspective. When each frequency component propagates with a different frequency, the initial step of traveling wave becomes distorted. Therefore, when the traveling wave propagates through a distance on power line, it will be leaned, which is called the dispersion of traveling waves.

3.5 Modal Transform

To divide aerial and ground mode, modal transforms is in use for different power system applications. In order to reach modal components, there are different transforms such as symmetrical component, the Clark, Karrenbauer and Wedephol [10]. The most common modal transform is the symmetrical component; however, it can only be applied to phase voltage and current versus the traveling waves which are instantaneous values. To carry out modal analysis on traveling waves there are other suitable methods, where although the result of these transforms are the same but in most studies, Clark transform is used for its superiority in transient study and its accessibility in different power system simulation software. The Clark transform operation for phase currents is indicated below:

$$\begin{bmatrix} I_0 \\ I_\alpha \\ I_\beta \end{bmatrix} = \frac{1}{3} \begin{bmatrix} 1 & 1 & 1 \\ 2 & -1 & -1 \\ 0 & \sqrt{3} & -\sqrt{3} \end{bmatrix} \begin{bmatrix} I_A \\ I_B \\ I_C \end{bmatrix} \quad (3.53)$$

where i_0 provides the ground mode and i_1 and i_2 provide the aerial modes phase currents [11]. Also in most of the studies, current traveling waves were applied for analyzing the traveling waves as described in [12] and [13], due to its advantage for making an easier measurement compared to voltage traveling waves.

3.6 Traveling Wave Fault Location

Traveling wave fault location methods are generally based on traveling waves' arrival time. At the onset of fault, the traveling will be generated and moves along the power line to the local and remote terminal. The arrival time difference between these traveling waves is the basis for traveling wave fault location methods. In order to comprehend the traveling wave logics, the lattice diagram which is the schematic representation of traveling waves arrival time can be found in Figure 3.

3.6.1 Single-ended Method

The traveling wave method could be single-ended or double-ended. The single-ended method utilizes the traveling waves captured at the local terminal to find the fault location. In this method, the time difference between the arrival time of the first and second

traveling wave seen at the local terminal will be used to estimate the fault location. The single-ended method can be applied to any transmission lines, it does not require any communication channel and its implementation is simple. However, its accuracy is less than the double-ended method. Also, dividing traveling waves from the faults and the reflected ones from other transmission lines are kind of a challenge. To determine the fault location, two equations could be written based on the arrival time of traveling waves as it follows:

$$m = (t_{L1} - t_f)v \quad (3.54)$$

$$3m = (t_{L2} - t_f)v \quad (3.55)$$

where t_{L1} and t_{L2} are the first and second traveling waves captured at local terminal, t_f is the time of fault incident, m is the fault location in km , v is the traveling waves propagation velocity and l is the line length. Finally, by using (3.54) and (3.55) the fault location could be found based on the arrival time of the first and second traveling wave at the local terminal as detailed below:

$$m = \left(\frac{t_{L2} - t_{L1}}{2}\right)v \quad (3.56)$$

3.6.2 Double-ended Method

In contrast, the double-ended method employs the traveling waves captured at the local and remote terminal to find the fault location. The double-ended method need for communication channel, restricts its capabilities and increases its cost. In the current method, fault location can be found again by writing two equations where these ones are based on the arrival time of the first traveling waves captured at the local and remote terminal (t_{L1} and t_{R1}) [13, 14].

$$m = (t_{L1} - t_f)v \quad (3.57)$$

$$l - m = (t_{R1} - t_f)v \quad (3.58)$$

Finally, using (3.57) and (3.58) the fault location could be derived as:

$$m = \frac{1}{2}[l - (t_{L1} - t_{R1})v] \quad (3.59)$$

3.7 Traveling wave fault protection

Fault protection applications of traveling waves have been recently considered due to a need for high speed and secure protection. The traveling wave fault protection methods can be sorted once again into two general categories, the double-ended and the single-ended method. The most general criteria which are on the same hand secure are the traveling waves arrival time and polarity. The arrival time of traveling waves could be found based on the equations for traveling wave fault location. However, it is not the same for polarity, as the polarity of traveling waves change because of the discontinuities on the transmission line [15, 16].

3.7.1 Single-ended Method

The single-ended method based on traveling waves arrival time, works based on the first and second traveling wave captured at the local terminal. If the time difference between these two captured traveling waves is equal to the time required by the traveling wave to travel the transmission line length and return to the local terminal, then there is an external fault where the equations for arrival time could be written as:

$$t_{L2} - t_{L1} = \frac{2L}{v} \quad (3.60)$$

In case the fault is internal, the arrival time difference for traveling wave captured at the local terminal will be lower than the time needed to travel the transmission line length twice. It can be mentioned as:

$$t_{L2} - t_{L1} < \frac{2L}{v} \quad (3.61)$$

Finally, if there is no traveling wave, then there will be no fault on the transmission line. This will be quite a challenge as fault happening at voltage zero crossing does not result in traveling waves and more than that, the breaker operation and some switching devices can result in traveling waves which makes it in need of schemes to separate these traveling waves from traveling waves as a result of fault [17]. Accordingly, these facts emphasize the need for back up protection for any traveling wave protection device.

3.7.2 Double-ended Method

For the double-ended method, the basic idea of using arrival times will be the same but the arrival time of first traveling waves captured at the local and remote terminal will be considered this time. In this case, the direction of external faults could be specified too. For the external fault in a positive direction, the arrival time difference of traveling waves for a transmission line with the length of l and propagation velocity of v will be as follows:

$$t_{L1} - t_{R1} = \frac{L}{v} \quad (3.62)$$

where t_{L1} is the arrival time of first traveling wave arriving at local terminal and t_{R1} is the arrival time of first traveling wave captured at remote terminal. In this case, this time difference will be equal to the time required for traveling wave to propagate from the remote terminal to the local terminal. However, for the external fault in the negative direction as the traveling wave will be first revealed at the local terminal, the difference between the arrival time of first traveling wave at the local and remote terminal will be as follow:

$$t_{L1} - t_{R1} = -\frac{L}{v} \quad (3.63)$$

which will be equal to the required time for traveling wave to propagate from the local terminal to the remote terminal. Eventually, for an internal fault, the difference between the arrival time of these traveling waves should be less than the time needed for the traveling waves to pass through the transmission line length, which can be demonstrated as:

$$|t_{L1} - t_{R1}| < \frac{L}{v} \quad (3.64)$$

As discussed previously, the polarity of traveling waves will be affected by discontinuities. The polarity difference for current and voltage traveling waves in double-ended protection is demonstrated in the following Table 2, where the traveling wave was indicated as a superimposed component.

Based on what is demonstrated in Table 2, if the polarity of the voltage traveling wave captured at local and remote terminal are the same, the fault will be internal and if it's not, the fault will be an external fault, as the polarity of one of the captured traveling waves will be due to the passing through the terminal discontinuity. The polarity of the traveling wave cannot be solely applied as a criterion to implement the traveling wave protection.

TABLE 2:
TRAVELING WAVE PROTECTION LOGIC USING TRAVELING WAVES
POLARITY

Fault Location	Superimposed Voltage Polarity	Local Terminal		Remote Terminal	
		Voltage	Current	Voltage	Current
Internal Fault	+	+	-	+	-
	-	-	+	-	+
External Fault in Positive Direction	+	+	-	+	+
	-	-	+	-	-
External Fault in Negative Direction	+	+	+	+	-
	-	-	-	-	+

However, it can be employed with the arrival time method to improve the security and reliability of the protection method [18, 19].

3.8 Summary

In the presented chapter, the theory of traveling wave was discussed briefly. The traveling wave equations obtained and the parameters affecting attenuation and dispersion were explained as well. Further, the traveling waves behavior at discontinuous such as bus, line termination and also fault location itself were described. In sum, the main applications of traveling waves in the power system was considered and the single-ended and double-ended methods with their formulation were provided.

Chapter 4

Traveling Waves Attenuation after Auto-reclosure

To reach a high-speed protection after auto-reclosure traveling wave method is the best as it's the fastest method available. After auto-reclosure, traveling wave transients will generate by breaker operation whether there is a fault on a power line or not. This makes the use of available traveling waves techniques such as arrival time or polarity different from the normal condition. As a result, considering the advantage of traveling wave protection and the need for high-speed protection, this chapter proposes a new auto-reclosure protection method based on traveling waves attenuation. The double-ended method will be used for simulation and to show the attenuation phenomena on traveling waves.

4.1 Proposed Solution

After auto-reclosure traveling waves will be generated due to breaker operation. To extract these high-frequency components the combination of series of high pass and low pass filters has been used in this literature which results in a simpler calculation and high accuracy results. The traveling wave due to breaker operation can be first seen at the local terminal. Then this traveling wave will move to the other end of the line and it will be attenuated during it's journey, which the degree of attenuation can be measured by the remote terminal relay [20]. In order to accurately capture the traveling wave arriving at remote terminal, the arrival time of traveling wave at remote terminal t_R which illustrated in Figure 4 can be used.

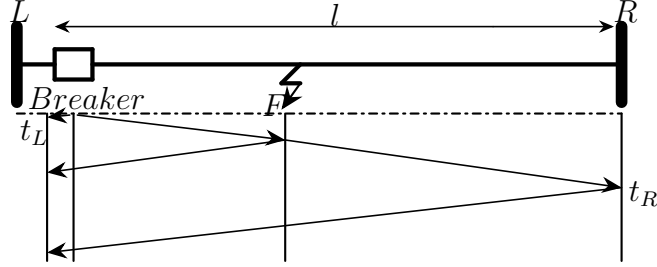


Figure 4: Bewley lattice diagram after auto-reclosure on a permanent fault

In high-speed auto-reclosure, as both local and remote terminal breakers operate with low time difference, the traveling waves caused by the local breaker operation may coincide with the traveling wave as a result of remote breaker operation or traveling wave reflection from adjacent buses. These phenomena make it hard to identify the traveling waves arriving at remote terminal. As a result, using Figure 4 which is providing the bewley lattice diagram for the traveling waves after auto-reclosure, the arrival time of traveling wave generated by the local breaker at remote terminal (t_R) could be calculated as follows:

$$t_R = \frac{l}{v} + t_L \quad (4.1)$$

where t_L is the time of local breaker operation, l is the line length and v is the propagation velocity, which as noted in chapter three could be expressed as:

$$v = \frac{1}{\sqrt{LC}} \quad (4.2)$$

where L is the inductance and C represents the capacitance of the transmission line [11].

The traveling wave reaching remote terminal at t_R is attenuated and dispersed due to the effect of transmission line characteristic impedance and it's length. As the transmission line impedance will be different for the permanent and temporary fault conditions, the presence of fault in case of permanent fault results in a different amount of attenuation for traveling waves compare to normal condition where fault has been extinguished. To compare these two conditions the theory has been developed as follow. In case of the temporary fault, as fault will extinguish after auto-reclosure then the traveling waves attenuation and dispersion as discussed in [21] will be only affected by the transmission line characteristic impedance.

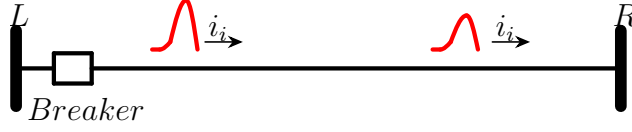


Figure 5: Traveling wave attenuation after successful auto-closure

To find the amount of this attenuation and dispersion as a result of characteristic impedance of the transmission, γ should be first defined. γ is the propagation constant, related to impedance and admittance of the transmission line as shown in (4.3) [22].

$$\gamma = \alpha + j\beta = \sqrt{ZY} \quad (4.3)$$

where, α provide the attenuation constant of the line. As discussed in [14] and later chapter, especially in three phase systems the modal analysis should be used to obtain the decoupled modes of traveling waves in order to remove mutual effect of phases on each other. Figure 5 provide the schematic of traveling waves attenuation due to line impedance where traveling wave as a result of auto-reclosure is attenuated during its travel to the remote terminal. The attenuation for traveling waves as a result of line impedance will be constant in case of successful auto-reclosure where the fault has been extinguished after de-energizing the power line.

In case of a permanent fault, the traveling wave will be attenuated by transmission line impedance and also due to boundary condition of waves at the fault point. Based on the traveling wave propagation phenomena at every fault point, the part of the traveling wave will be reflected and the other part will be transmitted. The magnitude of the reflected and the transmitted wave will be smaller than the magnitude of the incident wave [23, 24]. As a result, in this case the attenuation will be higher as it will be the sum of attenuation as a result of line impedance and also fault point. In the three-phase lines, the amount of attenuation will be different for every fault types.

As symmetrical faults are mostly permanent auto-reclosure does not take place for these kind of faults. However, in the case of unsymmetrical faults where the auto-reclosure take place, the reflected and transmitted waves in three phases are mutually coupled which means that there is a coupling phenomenon between traveling waves at the point of fault. In this situation first, the phase domain system should be decoupled into their modal components. As discussed in chapter three to extract modal components Clark transform

will be used due to its superiority in transient studies. The Clark transform to decouple phase currents is as follows:

$$\begin{aligned} I_0 &= \frac{(I_A + I_B + I_C)}{3} \\ I_\alpha &= \frac{(2I_A - I_B - I_C)}{3} \\ I_\beta &= \frac{\sqrt{3}(I_B - I_C)}{3} \end{aligned} \tag{4.4}$$

where I_0 is ground mode and I_α and I_β providing the aerial modes currents [11]. As an example, the reflection and transmission of traveling waves at AG fault point have been considered as shown in Figure 6. When phase A to ground fault occur, the transmission line will be divided in two sections. Section 1 can be considered from local terminal to fault point and section 2 will be the part from fault point to remote terminal. Assuming the traveling wave due to breaker operation will flow from section 1 to section 2 and also considering that there will be no backward traveling wave at section 2, which conform with the case the traveling wave arriving from local terminal and hitting the fault point for the first time, using waves boundary condition at fault point and the fact that there is only one current and voltage which can exist at fault point F , following equations could be written for voltage and current as:

$$e + e_r = e_t \tag{4.5}$$

$$i + i_r = i_t + [i_R \ 0 \ 0]^T \tag{4.6}$$

$$e = Zi \tag{4.7}$$

$$e_r = -Zi_r \tag{4.8}$$

$$e_t = Zi_t \tag{4.9}$$

$$e_{ta} = i_R R \tag{4.10}$$

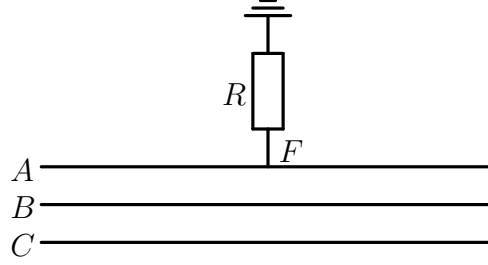


Figure 6: Phase A to ground fault by resistance R

where,

$Z = \begin{bmatrix} Z_s & Z_m & Z_m \\ Z_m & Z_s & Z_m \\ Z_m & Z_m & Z_s \end{bmatrix}$ is the wave impedance matrix of the line; $e = [e_a \ e_b \ e_c]^T$, $i = [i_a \ i_b \ i_c]^T$ are the incident voltage and current traveling waves. $e_r = [e_{ra} \ e_{rb} \ e_{rc}]^T$, $i_r = [i_{ra} \ i_{rb} \ i_{rc}]^T$ are the reflected voltage and current traveling waves and $e_t = [e_{ta} \ e_{tb} \ e_{tc}]^T$, $i_t = [i_{ta} \ i_{tb} \ i_{tc}]^T$ are the transmitted or refracted voltage and current traveling waves. i_R is the current flowing into resistance R. Premultiplying sides of the equation for the current traveling wave at fault point, combining it with the voltage of traveling waves at fault point and using the voltage and currents connecting by Z will result in:

$$e - e_r = e_t + Z [i_R \ 0 \ 0]^T \quad (4.11)$$

and again using voltage traveling wave equation at fault point,

$$2e_r = -Z [i_R \ 0 \ 0]^T \quad (4.12)$$

where according to the first line of this equation, $2e_{ra} = -Z_s i_R$ is obtained. Connecting it to the first line of voltage traveling wave equation at fault point will result in:

$$e_{ra} = -\frac{Z_s e}{Z_s + 2R} \quad (4.13)$$

Moreover, the reflected traveling wave on phase b and c can be found as:

$$e_{rb} = -\frac{Z_m e}{Z_s + 2R} \quad (4.14)$$

and,

$$e_{rc} = -\frac{Z_m e}{Z_s + 2R} \quad (4.15)$$

Z_0 and Z_1 are the wave impedance of zero and aerial modes which are given by:

$$Z_0 = Z_s + 2Z_m \quad (4.16)$$

and,

$$Z_1 = Z_s - Z_m \quad (4.17)$$

Using Clark phase-mode transformation formula and using the zero and aerial mode impedance will provide the reflected traveling waves for each mode as:

$$\begin{aligned} e_{\alpha r} &= \frac{-2Z_1(e_\alpha + e_0)}{2Z_1 + Z_0 + 6R} \\ e_{\beta r} &= 0 \\ e_{0r} &= \frac{-Z_0(e_\alpha + e_0)}{2Z_1 + Z_0 + 6R} \end{aligned} \quad (4.18)$$

where based on (4.5) the transmitted traveling waves can be found as:

$$\begin{aligned} e_{\alpha t} &= \frac{Z_0 + 6R}{2Z_1 + Z_0 + 6R} e_\alpha - \frac{2Z_1}{2Z_1 + Z_0 + 6R} e_0 \\ e_{\beta t} &= e_\beta \\ e_{0t} &= -\frac{Z_0}{2Z_1 + Z_0 + 6R} e_\alpha + \frac{2Z_1 + 6R}{2Z_1 + Z_0 + 6R} e_0 \end{aligned} \quad (4.19)$$

where the transmitted and reflected traveling wave equation for instance $e_{\alpha r}$ and $e_{\alpha t}$ consist of the aerial and zero component of incident waves (e_α and e_0) [25, 26]. As a result, the traveling wave attenuation for each mode due to the unsymmetrical fault will be different.

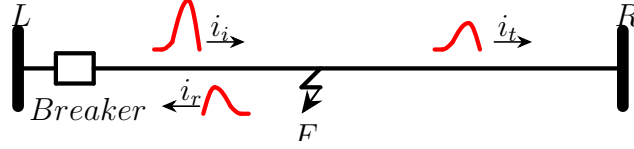


Figure 7: Traveling wave attenuation after auto-reclosure on permanent fault

In this study current traveling waves have been used as the current transformers (CTs) poses adequate frequency bandwidth compared to the voltage transformers (VTs) which can not preserve high frequency transients [12, 27]. Based on the modal component which shown in (4.4) in some cases α component and in some other cases β component can provide attenuation based on the fault type. For instance, as shown in (4.20) for AG fault the β component does not show the attenuation as a result of fault point since the fault is on phase A and Clark transform remove phase A current from the β component calculation.

$$I_{\beta} = \frac{\sqrt{3}}{3}(I_B - I_C) \quad (4.20)$$

The same could be observed from (4.18) where reflected β current traveling wave as a result of AG fault is equal to zero. For BC fault it's vice versa and α component is not suitable. As shown in (4.21), it's not showing the attenuation since it removes the attenuation effect by the fault on BC phase as it sum up current traveling wave on phase B and C which are equal but are with different polarities, which means $I_B = -I_C$.

$$I_{\alpha} = \frac{1}{3}(2I_A - I_B - I_C) \quad (4.21)$$

Finally, as discussed in the later two paragraphs always one of the aerial modes can provide a reliable result, which means α or either β component can show the attenuation as a result of fault point. Based on it the attenuation of both aerial components of traveling wave should be calculated, where for α component the resulting attenuation can be written as:

$$A_{\alpha} = \frac{|i_{\alpha L} - i_{\alpha R}|}{|i_{\alpha L}|} \quad (4.22)$$

and attenuation for β component (A_{β}) is:

$$A_\beta = \frac{|i_{\beta L} - i_{\beta R}|}{|i_{\beta L}|} \quad (4.23)$$

where L means the signal at local and R means the signal at the remote terminal. To generalize the study and eliminating the need for identifying the fault type to use α or β component, OR based logic has been used to find out whether the fault has been extinguished or still exist after auto-reclosure. To do the comparison the threshold values for α component (M_α) and β component (M_β) has been considered, where M_α and M_β are the attenuation of α and β component of traveling wave when there is no fault on the transmission line. These parameters could be measured from the first energization of transmission line, as the attenuation factor of traveling wave, just like the propagation velocity of traveling wave, does not considerably change during time. As a result, using the attenuation criteria for traveling waves, the protection algorithm for auto-reclosure condition has been proposed as demonstrated in Figure 8.

Hybrid transmission line is another kind of lines which include both the overhead line and underground cable and are in use in some urban areas or in places such as rivers where overhead line usage is not applicable. In underground cables auto-reclosure is not a proper procedure as the fault in the underground cable is usually permanent; however, in a hybrid line consisting of mostly overhead line and a part of underground cable having successful auto-reclosure is more probable. In this situation timing method proposed in equation 4.1 to capture the right traveling wave is still applicable as it's not based on the traveling wave reflection. However, there are some differences from the case of the attenuation for the traveling waves on overhead lines. In these kinds of lines as shown in Figure 9 the junction between overhead and underground cable result in reflection and transmission of traveling waves, Which eventually result in higher traveling wave attenuation.

Considering the principles explained for the simple overhead line it can be concluded that the traveling wave attenuation by successful auto-reclosure on hybrid line will be the result of line attenuation and also the transmission coefficient of overhead and underground cable junction. As a result, in this situation, the attenuation of traveling waves on hybrid line will be higher than simple overhead line. However, the difference between the internal temporary and permanent fault is still easily distinguishable as the attenuation as a result of fault point still exist. Based on the traveling wave transmission theory as the hybrid line junction is for all three phases it will be symmetrical change in all phases. As a result, the reflection (i_r) and refraction or transmission (i_t) of the current traveling wave for the overhead and underground cable junction can be expressed as:

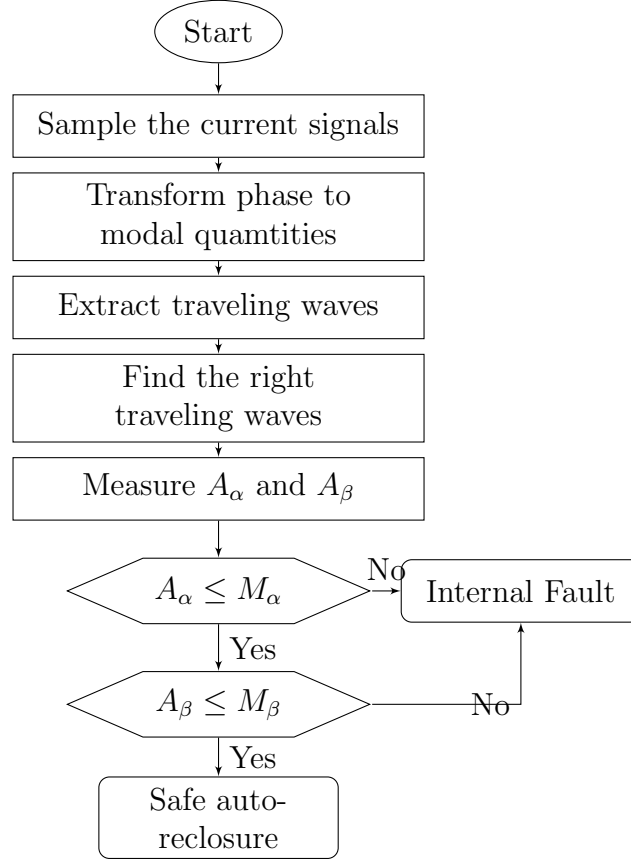


Figure 8: Proposed traveling wave based protection scheme for transmission lines after auto-reclosure

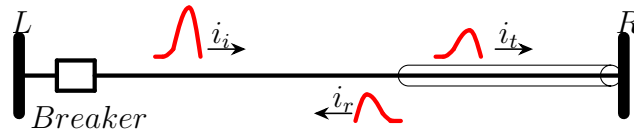


Figure 9: Traveling wave attenuation on hybrid line after successful auto-reclosure

$$i_t = \frac{e_t}{Z_t} = \left(\frac{-2}{Z_i + Z_t} \right) e_i \quad (4.24)$$

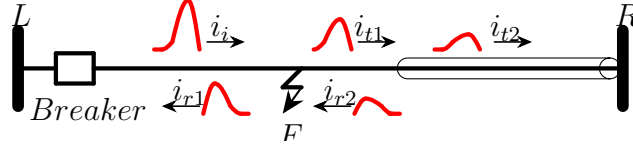


Figure 10: Traveling wave attenuation on hybrid line with permanent fault

$$i_r = -\frac{e_r}{Z_i} = \left(\frac{Z_i - Z_t}{Z_i + Z_t}\right) \frac{e_i}{Z_i} \quad (4.25)$$

where Z_i is the overhead line characteristic impedance and Z_t is the underground cable characteristic impedance [17, 19]. In case of a permanent fault on the hybrid transmission line the amount of attenuation will be different for each fault type and it will be the same as the equation 4.18 and 4.19. As a result the magnitude of traveling wave will be subjected to junction point attenuation, line attenuation and also the fault point; which, eventually result in higher attenuation compare to the case where the fault has been extinguished after auto-reclosure. Figure 10 provide schematic illustration of this phenomena and traveling wave successive reflection and attenuation due to fault point and hybrid line junction.

4.2 Performance Evaluation

Two power system model has been used for simulation and verifying the principles. First model consist of only overhead line; however, the hybrid system consist of mostly overhead line and small part of underground cable. Both models use the same power sources, however, line parameters differ widely as the underground cable transmission has been used in the hybrid system.

4.2.1 Overhead line

Simulations for an overhead line has been carried out for $230kV$, $100km$ transmission line where its schematic model illustrated in Figure 11 and electrical parameters described in Table 3.

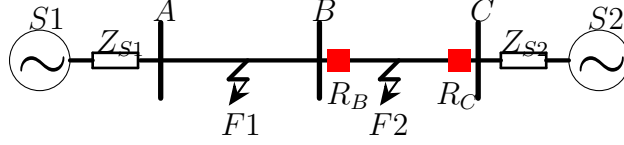


Figure 11: The 230-kV overhead line model

TABLE 3:
TRANSMISSION LINE ELECTRICAL PARAMETERS FOR OVERHEAD LINE

Data	Source 1		Source 2	
	Z (ohm)	$\angle Z$ (deg)	Z (ohm)	$\angle Z$ (deg)
Positive Sequence	23.09	82.87	12.66	81.87
Zero Sequence	16.163	82.87	11.094	81.87

Overhead Transmission Line				
Data	R (pu)	X (pu)	B (pu)	Surge Imp. (pu)
Positive Sequence	0.0067	0.0957	0.1732	0.7432
Zero Sequence	0.0678	0.2495	0.1231	1.4234

Temporary Fault

In case of temporary fault on the overhead line as explained in previous sections the traveling wave induced by breaker will not be reflected or transmitted. As a result, the attenuation of the traveling wave at the end of the line will be solely due to transmission line impedance. The traveling wave induced after successful auto-reclosure and captured at the remote terminal is shown in Figure 12, where relay B is located at local and relay C is at remote terminal.

The first traveling wave can be seen at relay B and the other will reach relay C after the time difference discussed in equation (4.1). Using (4.1), this time difference can be calculated as follow. Considering the propagation velocity of aerial mode traveling wave on this overhead line model which is $299851km/sec$. and line length of $100km$, the arrival time of traveling wave as a result of auto-reclosure at relay C will be $0.0003335sec$.

As a result, using this arrival time, the traveling wave caused by the breaker operation at local terminal (bus B) could be easily distinguished from noise or other traveling waves reaching remote terminal (bus C). Then after capturing the right traveling waves, as

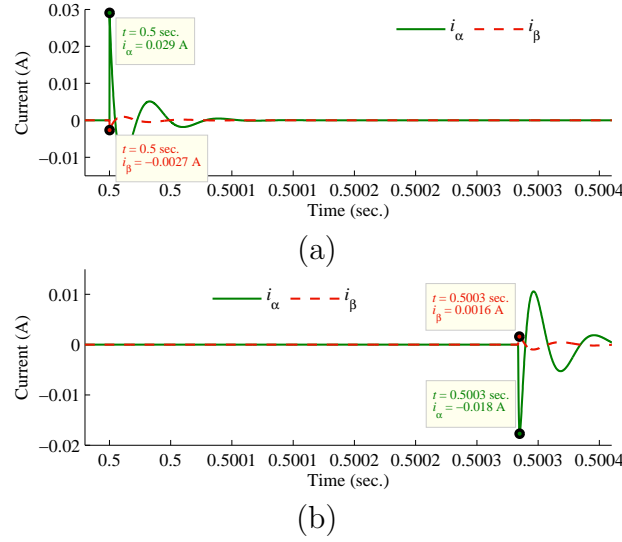


Figure 12: Current traveling waves of aerial modes after successful auto-reclosure on overhead line, (a) Traveling wave captured at relay B, (b) Traveling wave captured at relay C

explained the attenuation of the α component of the current traveling wave reaching relay C, can be calculated. Using (4.22) and the samples pinpointed in Figure 12, the attenuation for α component will be 39.04%. Similarly, using (4.23) and the samples pinpointed in Figure 12 the attenuation for β component will be 39.29%

To distinguish between temporary and permanent fault, the attenuation of α and β component of current traveling waves due to line characteristic impedance has been used as threshold value (M). As a result in this study M_α and M_β will be:

$$M_\alpha = A_\alpha = 39.04\%$$

$$M_\beta = A_\beta = 39.29\%$$

Permanent Fault

In the case of an internal permanent fault, the traveling wave will be affected by the fault. For simulation purposes AG fault has been generated at 70km away from the local terminal

with the fault resistance of 1Ω . This case results in reflection and transmission of traveling waves at fault point. The traveling wave seen at end of the line for this fault has been shown in Figure 13, where the traveling wave arrival time is exactly the same as successful auto-reclosure. Using (4.22) and (4.23), the samples pinpointed in Figure 13 results in $A_\alpha = 74.14\%$ and $A_\beta = 39.29\%$. The amount of attenuation for α component of the current traveling wave is higher than the threshold value due to fault point attenuation. As a result, the permanent fault could be detected using the attenuation in the α component of the current traveling wave; however, the same is not true for the amount of attenuation for the β component of the current traveling wave as discussed in (4.20). The attenuation of β component of current traveling wave should be measured as in some fault types such as BC fault, the amount of attenuation for α component is the same as threshold value. The simulation analysis has been carried out for internal BC fault in order to measure the amount of attenuation for aerial component of current traveling wave and results has been provided in Figure 14.

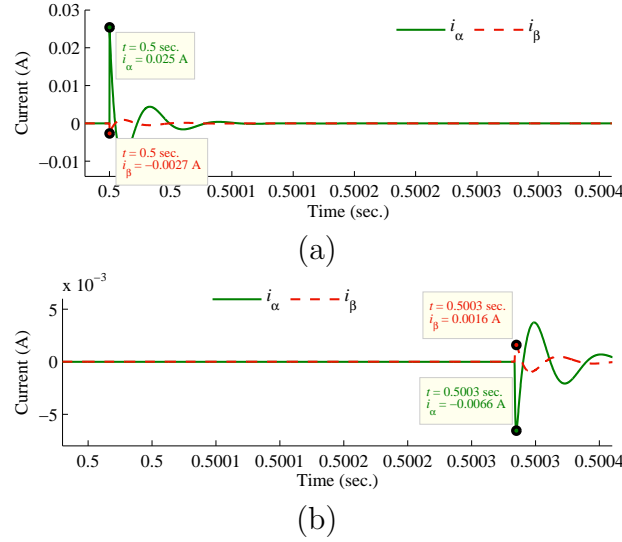


Figure 13: Current traveling waves of aerial modes for internal AG fault of overhead line, (a) Traveling wave captured at relay B, (b) Traveling wave captured at relay C

Using equations (4.22) and (4.23), the samples pinpointed in Figure 14 results in $A_\alpha = 39.04\%$ and $A_\beta = 99.79\%$, where α component attenuation is the same as the threshold value and β component attenuation can be used for fault detection. As a result, the traveling wave attenuation due to fault can always be detected using either α or β component.

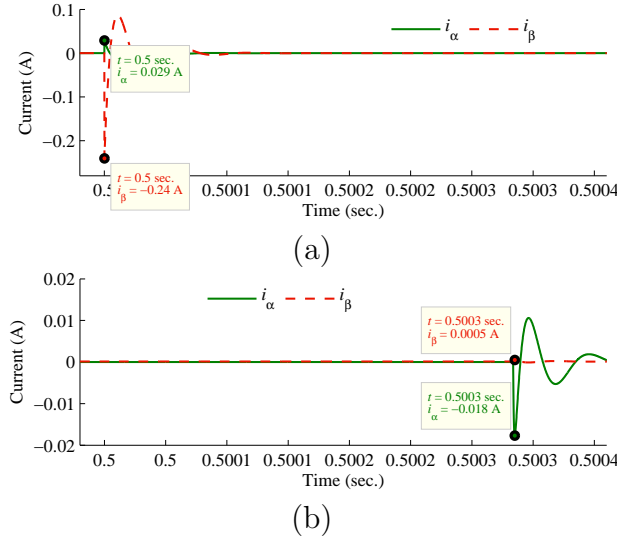


Figure 14: Current traveling waves of aerial modes for internal BC fault of overhead line, (a) Traveling wave captured at relay B, (b) Traveling wave captured at relay C

External Fault

In case auto-reclosure is successful but there is another fault on adjunct line, which is the transmission line between bus A and B , the magnitude of traveling waves will be different from successful auto-reclosure. However, as the fault is external there is no reflection or transmission for the traveling wave reaching to relay C . As a result, the attenuation of α and the β component will be the same as the threshold value (M). In this case, an external AG fault has been applied at 70km away from relay B on the adjacent line. The traveling wave attenuation for this case is shown in Figure 15.

Using the pinpointed data in Figure 15 and equations (4.22) and (4.23) the attenuation in the α and β component of the current traveling waves are $A_\alpha = 39.14\%$ and $A_\beta = 39.29\%$, which as expected are the same as threshold value (M).

4.2.2 Hybrid-line System

Simulation for the hybrid line has been carried out using the mix of overhead line and underground cable. The schematic model for this system has been shown in Figure 16 where an overhead line is 95km , and 5km of underground cable is located at the end of the

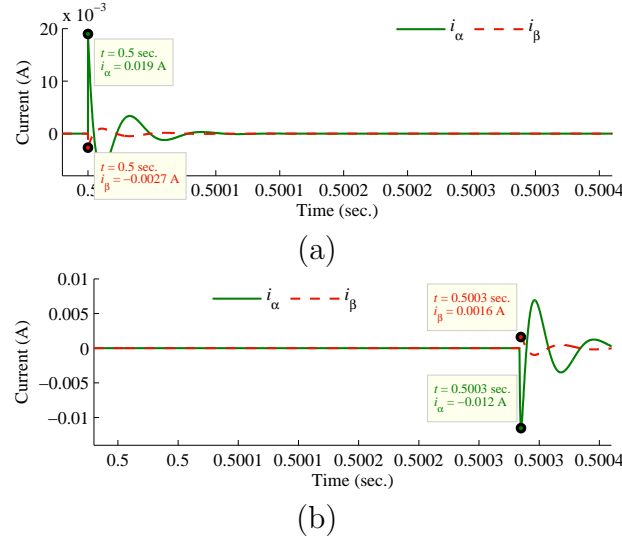


Figure 15: Current traveling waves of aerial modes for an external AG fault of overhead line, (a) Traveling wave captured at relay B, (b) Traveling wave captured at relay C

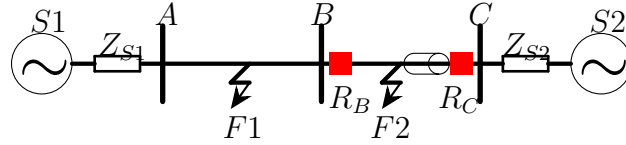


Figure 16: The 230-kV hybrid-line system model

line. In underground cable simulated here, the cable attenuation is higher compared to the overhead line, as a result, the amount of attenuation for traveling waves which consists of attenuation as a result of line impedance and hybrid line intersection will be higher than the overhead line simulation case. However, the difference between internal fault and no fault condition or external fault is still easily noticeable.

In this case, power sources are the same as the overhead line parameters provided in Table 3; however, the overhead line electrical parameters are different due to the different line length. These parameters are elaborated along with underground cable electrical parameters in Table 4.

TABLE 4:
TRANSMISSION LINE ELECTRICAL PARAMETERS FOR HYBRID-LINE SYSTEM

Overhead Transmission Line				
Data	R (pu)	X (pu)	B (pu)	Surge Imp. (pu)
Positive Sequence	0.0063	0.0909	0.1645	0.7433
Zero Sequence	0.0645	0.2372	0.1169	1.4239

Under Ground Cable				
Data	R (pu)	X (pu)	B (pu)	Surge Imp. (pu)
Positive Sequence	0.0013	0.0014	0.3886	0.0605
Zero Sequence	0.0018	0.0007	0.3886	0.0442

Temporary Fault

Traveling wave attenuation and arrival time for the temporary fault on hybrid-line are shown in Figure 17.

In hybrid line, the arrival time of traveling waves from the breaker at bus B to the relay C could be calculated in the same way it's done for an overhead line model. However, the traveling wave propagation speed is different and it's equal to $285303km/sec.$, for $100km$ of hybrid underground and overhead line. As a result, using (4.1) and the mentioned parameters such as line length and traveling wave propagation velocity through over head line, the arrival time of traveling waves at remote terminal (bus C) is equal to $0.5003505sec.$ Similarly to the case of over head line, the attenuation of current traveling wave captured after auto-reclosure at remote terminal could be calculated. Using equations (4.22) and (4.23), the samples pinpointed in Figure 17 results in $A_\alpha = 91.48\%$ and $A_\beta = 91.56\%$. As a result the threshold value for α and β component will be:

$$M_\alpha = A_\alpha = 91.48\%$$

$$M_\beta = A_\beta = 91.56\%$$

which will be used in the next sections to carry out comparison in the attenuation of traveling waves after successful and unsuccessful auto-reclosure on a hybrid-line system.

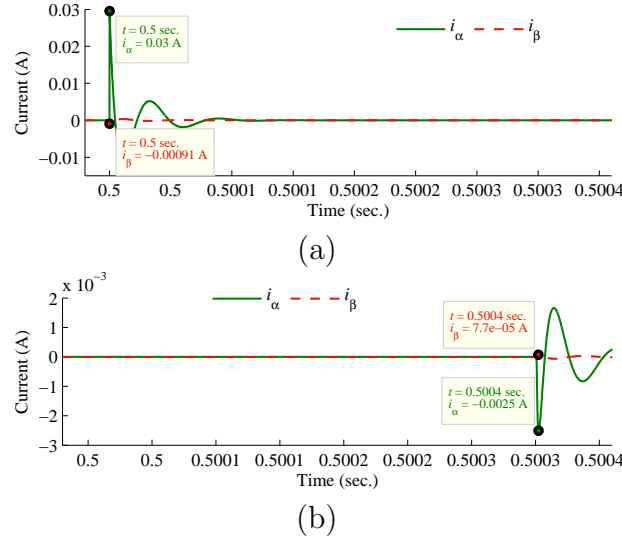


Figure 17: Current traveling waves of aerial modes after successful auto-reclosure on hybrid-line system, (a) Traveling wave captured at relay B, (b) Traveling wave captured at relay C

Permanent Fault

As illustrated in Figure 18, during an internal fault, the α and β component attenuation should be higher than a threshold value (M). Using the pinpointed samples in Figure 18 and equation (4.22) and (4.23), the α and β component traveling wave attenuation could be written as $A_\alpha = 96.34\%$ and $A_\beta = 91.95\%$.

As a result, the permanent fault could be recognized by comparing the threshold value with current traveling wave attenuation. However, as discussed both α and β component attenuation should be calculated. To show the situation in hybrid-line that the calculation of both components is necessary, BC internal fault has been created on the hybrid-line model where the attenuation of traveling waves could be seen in Figure 19.

Using the samples pinpointed in Figure 19, equation (4.22) and (4.23) the higher attenuation caused by fault results in $A_\alpha = 91.48\%$ and $A_\beta = 99.92\%$, where just the β component attenuation reflecting the effect of fault.

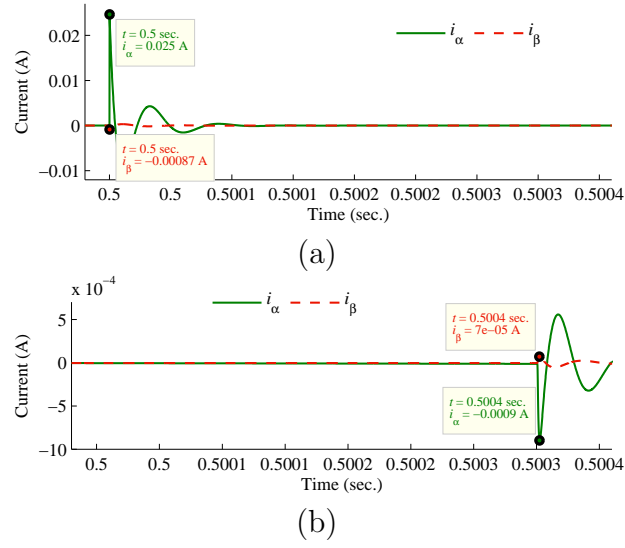


Figure 18: Current traveling waves of aerial modes for internal AG fault of hybrid-line system, (a) Traveling wave captured at relay B, (b) Traveling wave captured at relay C

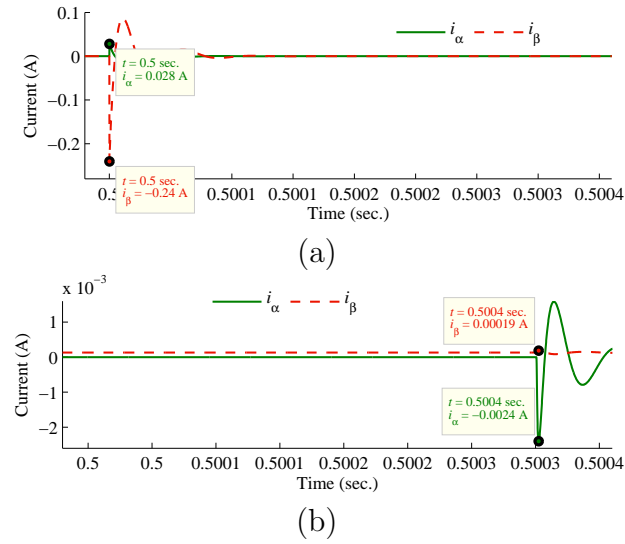


Figure 19: Current traveling waves of aerial modes for internal BC fault of hybrid-line system, (a) Traveling wave captured at relay B, (b) Traveling wave captured at relay C

External Fault

Attenuation in external fault condition will be the same as no fault condition as there is no attenuation due to fault in the traveling wave path to reach the other end of the line. The attenuation for AG external fault has been shown in Figure 20, where the attenuation percentage using (4.22), (4.23) and pinpointed samples could be written as $A_\alpha = 91.51\%$ and $A_\beta = 91.71\%$, which is as expected, is the same as attenuation in no fault condition.

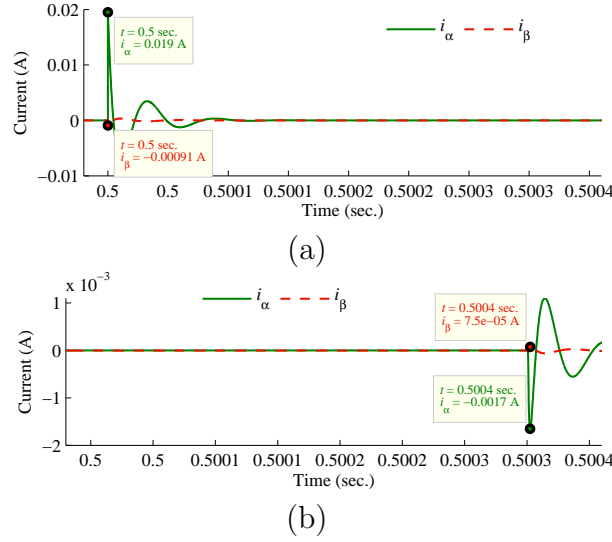


Figure 20: Current traveling waves of aerial modes for external AG fault of hybrid-line system, (a) Traveling wave captured at relay B, (b) Traveling wave captured at relay C

4.2.3 Effect of Fault Resistance

Scheme evaluation is carried out on a $230kV$, $100km$ transmission line using the overhead line model parameters elaborated in Table 3, where fault resistance, fault location, line length, frequency effect and fault type effect are investigated. In high impedance faults, traveling waves will become weaker and their detection is difficult. However, the attenuation difference could still be seen. In this case considering (4.19), higher fault resistance will result in less attenuation. However, this attenuation should never fall below the threshold value to detect an internal fault. As a result, simulation scenarios with different fault resistance has been used. As illustrated in Figure 21 there is a secure margin between the internal fault and the external fault even for very high impedance faults.

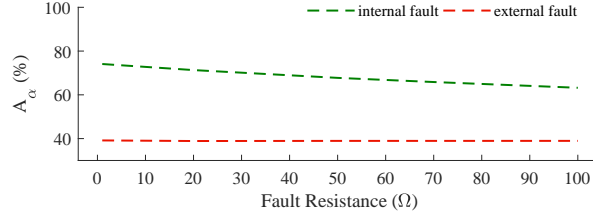


Figure 21: Fault resistance effect for internal and external AG fault

4.2.4 Effect of Fault Type

The performance of the proposed scheme evaluated for different fault types. Table 5 provide information on the α and β component attenuation for different fault types, where the difference between the magnitude of the traveling wave induced by breaker action for the no-fault and internal fault case can be noticed.

In Table 5, $i_{\alpha A}$ and $i_{\beta A}$ indicating the magnitude of aerial modes of the current traveling captured at local terminal and $i_{\alpha B}$ and $i_{\beta B}$ indicating the magnitude of aerial modes of the current traveling waves captured at remote terminal. A_α and A_β are providing the attenuation of these traveling waves, which in the case of permanent fault at least one of these parameters are always more than the one calculated for no fault condition or healthy line. As discussed, the need for both α and β component attenuation is noticeable throughout the Table 5. In some faults such as BG fault the attenuation of traveling waves for both of the α and β components can be used, in AG fault just the α component can be used and in BC fault the β component attenuation provide the result. However, it's important that in all these conditions the attenuation of the α or β component can be used as a sign of permanent fault. Also, the small difference between the attenuation of α and β component for other fault types can be explained considering the different transmission coefficient for each fault type. Also, it can be seen that for unsymmetrical internal faults the attenuation of α and β component traveling waves are different from each other which is understandable considering the difference in reflected α and the β component which have shown in (4.18). However, for symmetrical faults as discussed the attenuation of both components will be the same.

4.2.5 Effect of Fault Location

Fault location can change the fault point which can change the attenuation due to equation (4.18). However, its attenuation is not comparative to the attenuation as a result of line

TABLE 5:
PROPOSED SCHEME UNDER DIFFERENT FAULT TYPES

Fault type	Fault specification	Relay A		Relay B		Attenuation (%)	
		$i_{\alpha A}(A.)$	$i_{\beta A}(A.)$	$i_{\alpha B}(A.)$	$i_{\beta B}(A.)$	A_{α}	A_{β}
Healthy line	-	0.02894	-0.00264	-0.01772	0.00160	38.77%	39.03%
AG	Internal	0.02532	-0.00264	-0.00656	0.00160	74.08%	39.03%
	External	0.01896	-0.00264	-0.01153	0.00160	39.16%	39.03%
BG	Internal	0.08112	-0.09300	-0.02827	0.01988	65.14%	78.61%
	External	-0.03267	0.10419	0.01996	-0.06365	38.9%	38.9%
CG	Internal	-0.02505	-0.09618	-0.00159	0.02955	93.64%	69.27%
	External	0.08577	0.09560	-0.05231	-0.05830	39.01%	39.01%
ABG	Internal	0.09437	-0.09029	0.00662	0.01243	92.97%	86.22%
	External	-0.05461	0.10149	0.03335	-0.06193	38.92%	42.36%
ACG	Internal	-0.06743	-0.10851	-0.01338	0.02398	80.15%	77.89%
	External	0.10090	0.10236	-0.06152	-0.06245	39.02%	38.98%
BCG	Internal	0.02935	-0.23905	-0.01338	0.00088	54.39%	99.66%
	External	0.02230	0.23578	-0.01361	-0.14430	38.94%	38.8%
ABCG	Internal	0.00795	-0.23987	0.000043	0.00088	99.45%	99.63%
	External	0.02339	0.23643	-0.01423	-0.14436	39.15%	38.94%
AB	Internal	0.11248	-0.05098	-0.00396	-0.00633	96.47%	87.58%
	External	-0.07665	0.05842	0.04682	-0.03564	38.92%	38.99%
AC	Internal	-0.09240	-0.07292	-0.00492	0.00899	94.66%	87.67%
	External	0.13088	0.05615	-0.07983	-0.03424	39%	39.01%
BC	Internal	0.02894	-0.23924	-0.01771	0.00050	38.78%	99.78%
	External	0.02894	0.23622	-0.01772	0.14461	38.78%	38.77%
ABC	Internal	0.00234	-0.24004	0.000017	0.00037	99.23%	99.84%
	External	0.02746	0.23699	-0.01670	-0.14471	39.16%	38.93%

impedance, except in close in faults where the fault point effects is higher. As a result, different fault location has been considered for simulation study. As illustrated in Figure 22, there is a secure margin between the amount of attenuation for external and internal fault, where the attenuation is constant for any external fault. In close-in faults, the difference between the external and internal fault detection will be lower; however, it's still distinguishable. Moreover, Table 6 provide the effect of fault location for different

fault types, where in all cases there is secure margin between internal and external fault conditions.

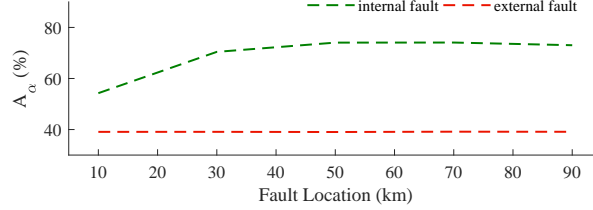


Figure 22: Fault location effect for internal and external AG fault

4.2.6 Effect of Line Length

Considering the effect of line impedance on the amount of traveling waves attenuation, it's clear that higher transmission line length will result in higher attenuation, which effects temporary and permanent fault condition in the same way. However, considering (4.18) the attenuation of traveling waves as a result of fault will be effected too, but its effect is low and it's not comparative to the attenuation as a result of line impedance. Different simulation has been performed to show that line length does not affecting the proposed fault detection scheme, where Figure 23 provide the simulation results for different transmission line length as follow.

4.2.7 Sensitivity of the Scheme to the Frequency

From the traveling wave equations, it can be seen that the traveling waves magnitude is dependent on the characteristic impedance of the line, which is affected by the power line frequency. Although the magnitude of the traveling wave is dependent on the power line frequency, this scheme is not affected by the frequency as it's based on the comparison of traveling wave magnitude at two different location. To show that, scheme performance has been investigated for two most common frequencies for power transmission lines, the 50 and 60 Hz. Table 7 provide result for α component attenuation for different line conditions, where it's relatively similar for different frequencies.

TABLE 6:
FAULT LOCATION EFFECT FOR DIFFERENT FAULT TYPES

Fault type	Fault location (<i>km</i>)	A_α (%)	A_β (%)	Analysis result
BG	30	65.91	80.47	Internal Fault
	50	65.03	79	Internal Fault
	70	65.14	78.61	Internal Fault
	-30	38.92	38.92	External Fault
	-50	39.01	39.02	External Fault
	-70	38.9	38.9	External Fault
BC	30	38.93	99.81	Internal Fault
	50	38.85	99.80	Internal Fault
	70	38.78	99.78	Internal Fault
	-30	38.93	38.94	External Fault
	-50	38.89	38.97	External Fault
	-70	38.78	38.77	External Fault
BCG	30	53.57	99.65	Internal Fault
	50	42.48	99.64	Internal Fault
	70	54.39	99.66	Internal Fault
	-30	38.90	38.94	External Fault
	-50	38.91	39.01	External Fault
	-70	38.94	38.80	External Fault
ABC	30	99.23	99.86	Internal Fault
	50	99.24	99.85	Internal Fault
	70	99.23	99.84	Internal Fault
	-30	39.10	38.93	External Fault
	-50	39.18	39	External Fault
	-70	39.16	38.93	External Fault
ABCG	30	99.48	99.65	Internal Fault
	50	99.47	99.64	Internal Fault
	70	99.45	99.63	Internal Fault
	-30	39.12	38.94	External Fault
	-50	39.19	39.01	External Fault
	-70	39.15	38.94	External Fault

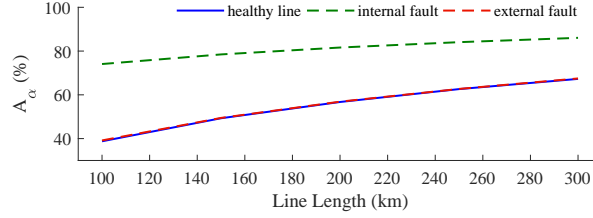


Figure 23: Transmission line length effect for healthy line, internal and external AG fault

TABLE 7:
SENSITIVITY OF THE SCHEME TO THE FREQUENCY BY EMPLOYING
ATTENUATION OF α COMPONENT

Frequency (Hz)	Healthy Line	Internal Fault	External Fault
50	38.91%	74.10%	39%
60	38.77%	74.08%	39.16%

4.2.8 Attenuation in the Energy of the Traveling Waves

As mentioned the one sample criteria for attenuation of traveling waves which is based on its magnitude, is not proper as it's so susceptible to noises on the transmission line. To improve its security, the three sample criteria has been considered too, which its program has been introduced in Appendix A. However, even three sample criteria can have a chance of getting through noises and reducing accuracy. As a result, this section provides the attenuation in the energy of traveling waves through its propagation on the power line and fault point. Table 8 provides the attenuation in the energy of traveling waves after successful and unsuccessful auto-reclosure, where $Ei_{\alpha A}$ and $Ei_{\beta A}$ is the energy of α and β current traveling wave seen at relay A, $Ei_{\alpha B}$ and $Ei_{\beta B}$ is the energy of α and β current traveling wave captured at relay B. EA_α and EA_β provide the attenuation in the energy of α and β component of captured traveling waves. As could be seen from Table 8, the attenuation of traveling waves for internal fault case is always higher than the attenuation for external fault or successful auto-reclosure. The gap between these two condition is also higher than attenuation in magnitude of traveling waves which is another good reason for using it beside of the magnitude attenuation criteria.

TABLE 8:
ATTENUATION IN THE ENERGY OF THE TRAVELING WAVES

Fault type	Fault spec.	Relay A		Relay B		Atten.(%)	
		$Ei_{\alpha A}$	$Ei_{\beta A}$	$Ei_{\alpha B}$	$Ei_{\beta B}$	EA_{α}	EA_{β}
Healthy line	-	1.07×10^{-6}	8.85×10^{-9}	0.79×10^{-6}	6.50×10^{-9}	26.04	26.57
AG	Internal	8.27×10^{-7}	8.85×10^{-9}	0.11×10^{-6}	6.49×10^{-9}	86	26.57
	External	4.55×10^{-7}	8.85×10^{-9}	0.33×10^{-6}	6.50×10^{-9}	26.29	26.57
BG	Internal	1.11×10^{-5}	8.46×10^{-6}	0.20×10^{-5}	9.83×10^{-7}	81.93	88.38
	External	1.36×10^{-6}	1.39×10^{-5}	1.01×10^{-6}	1.02×10^{-5}	26.01	26.01
CG	Internal	8.06×10^{-7}	1.18×10^{-5}	3.64×10^{-8}	2.16×10^{-6}	95.47	81.77
	External	9.38×10^{-6}	1.16×10^{-5}	0.69×10^{-5}	8.62×10^{-6}	26.06	26.05
BC	Internal	1.07×10^{-6}	7.35×10^{-5}	0.79×10^{-6}	7.74×10^{-10}	26.04	99.99
	External	1.07×10^{-6}	7.17×10^{-5}	0.79×10^{-6}	5.30×10^{-5}	26.04	26.04
ABC	Internal	7.93×10^{-9}	7.36×10^{-5}	1.83×10^{-12}	8.82×10^{-11}	99.97	99.99
	External	0.95×10^{-6}	7.18×10^{-5}	0.70×10^{-6}	5.31×10^{-5}	26.35	26.04

4.3 Conclusions

In this chapter, after auto-reclosure protection based on the traveling waves attenuation has been proposed and its performance has been verified by different simulation results on two different type of lines. Different factors affecting this method considered to evaluate its performance including fault type, fault resistance, fault location and transmission line length. To improve the performance and security both α and β component has been used and method based on arrival time of traveling waves has been proposed to detect the right traveling wave, where the result of all these simulations prove the security and practicality of this method for high-speed protection after auto-reclosure.

Chapter 5

Single-ended Traveling Wave Based Protection after Auto-reclosure

5.1 Proposed Solutions

In this chapter, the proposed solution for high-speed traveling wave-based protection after auto-reclosure using the traveling wave captured at local terminal will be presented. The solution consist of some well-known criteria for traveling wave protection such as polarity and arrival time. Although these criteria are well-known, the novelty of this research is concerned with proposing new methods based on these criteria for single-ended protection after auto-reclosure.

5.1.1 Polarity of Traveling Waves after Auto-reclosure

As discussed in Chapter Three, the polarity of traveling waves is affected by any discontinuity or termination on the power line. After auto-reclosure traveling waves are generated due to breaker operation. The polarity of these traveling waves is unknown; however, there will be two possibilities for its reflection. If the fault is permanent, it will continue to exist even after auto-reclosure. As a result, the reflection of traveling waves will be due to the fault before the remote terminal. In the other case where the fault is temporary and it has been removed after auto-reclosure, the traveling wave reflection will be as a result of remote terminal. In this case, the reflected voltage traveling wave will be due to symmetrical junction at remote terminal, which is called line termination. The magnitude of the reflected wave is based on voltage traveling wave coefficient which is as follow:

$$e_r = \frac{Z_L - Z_i}{Z_L + Z_i} e_i \quad (5.1)$$

where Z_i is the characteristic impedance of the transmission line or impedance seen by incident wave and Z_L is the load impedance at line termination. Considering that the remote end is grounded and load impedance is lower than the line characteristic impedance ($Z_L < Z_i$), the reflected voltage traveling wave from remote end will have the opposite polarity compared to incident voltage traveling wave. However, for the current traveling wave as its reflection coefficient is opposite to the voltage traveling wave reflection coefficient mentioned earlier, the reflected current traveling wave will have the same polarity compared to the incident current traveling wave. As mentioned, this junction is symmetrical, and the polarity change of the reflected traveling wave occurs for all phases. However, in the case of unsuccessful auto-reclosure, the polarity of reflected traveling wave will be different for each case of fault due to a different kind of faults and associated mutual impedance. In addition, the change in polarities on each phase will be different as the fault may not be symmetrical. In particular, the problem arises for symmetrical faults such as *ABC* and *ABCG* fault where the impedance seen by transmitted traveling wave (Z_t) is lower than the line impedance or the impedance seen by incident wave (Z_i). The reason behind it is that Z_t will be as a result of line impedance (Z_i) becoming parallel with fault resistance (R), which result in lower value than Z_i . Consequently, using (5.1), the polarity of reflected traveling waves after unsuccessful auto-reclosure on these faults will be the same as successful auto-reclosure case. However, this is not important as generally auto-reclosure does not carry out after symmetrical faults.

Similar logic can be written for the case of the transmission line that ends up to infinity impedance. The example of such a condition after auto-reclosure is the case where remote breaker is still open. In this case, again using (5.1) as the Z_L will be higher than Z_i ($Z_L > Z_i$), the remote end results in opposite polarity for reflected voltage traveling wave and the same polarity as the incident wave for reflected current traveling wave. However, the reflected traveling waves after unsuccessful auto-reclosure as a result of reflection by fault will not follow the same pattern. Moreover, the problem with symmetrical faults does not repeat in this case, as in symmetrical faults Z_t will be lower than Z_i but in the case of successful auto-reclosure Z_t , which is equal to Z_L , will be higher than the line impedance Z_i .

Keeping these in mind, using the polarity of traveling waves after auto-reclosure, logics has been proposed as follows. In case of auto-reclosure on transmission line with closed termination ($Z_L < Z_i$), when there is still fault on the power line after auto-reclosure, the polarity of reflected current traveling wave or the second traveling wave captured at local

terminal do not follow the expected polarity change for successful auto-reclosure on closed termination power line with $Z_L < Z_i$. This logic could be written as:

$$\begin{aligned} & \textit{For transmission line with closed termination } (Z_L < Z_i) \\ & \textit{Unsuccessful Auto-reclosure : } \Delta_{i1} \times \Delta_{i2} < 0 \end{aligned} \quad (5.2)$$

where Δ_{i1} and Δ_{i2} are the polarities of the first and second successive current traveling waves seen at the local terminal. It should be noted that this scheme is only true when the remote terminal breaker is closed, and Z_L is lower than Z_i . The same can be written for voltage traveling wave, where the polarity of the first and second traveling wave can provide information regarding transmission line status as follows:

$$\begin{aligned} & \textit{For transmission line with closed termination } (Z_L < Z_i) \\ & \textit{Unsuccessful Auto-reclosure : } \Delta_{e1} \times \Delta_{e2} > 0 \end{aligned} \quad (5.3)$$

where Δ_{e1} and Δ_{e2} are the polarity of the first and second successive voltage traveling waves seen at the local terminal.

For the case where local relay is the first relay to close and the transmission line is still open from the other end, the remote breaker is still open or the remote end is not grounded or Z_L is higher than Z_i , this scheme will change as follows:

$$\begin{aligned} & \textit{For transmission line with open termination } (Z_L > Z_i) \\ & \textit{Unsuccessful Auto-reclosure : } \Delta_{i1} \times \Delta_{i2} > 0 \end{aligned} \quad (5.4)$$

which means, when the polarity of successive traveling waves is the same, there is still fault on the power line. However, when the power line is open from one end, the relationship between the first and second traveling wave at the time of unsuccessful auto-reclosure could be written as:

$$\begin{aligned} & \textit{For transmission line with open termination } (Z_L > Z_i) \\ & \textit{Unsuccessful Auto-reclosure : } \Delta_{e1} \times \Delta_{e2} < 0 \end{aligned} \quad (5.5)$$

where again Δ_{e1} and Δ_{e2} are the polarity of the first and second successive voltage traveling waves seen at the local terminal. It should be noted that in most of the traveling wave protection methods, the current traveling wave is in use owing to the better frequency response of Current Transformers (CTs) versus Coupling Capacitor Voltage Transformer (CCVT) or the limited bandwidth of Voltage Transformers (VTs) [14]. However, in this

study, both the current and voltage traveling waves have been discussed, and protection methods have been proposed for each one separately as this issue may be resolved using better voltage measurement devices.

5.1.2 Arrival Time of Traveling Waves after Auto-reclosure

After auto-reclosure, there will be two possibilities for the arrival time of traveling waves. First, the arrival time of second traveling wave seen at the local terminal is equal to the travel time of traveling waves to propagate through the transmission line and returning to the local terminal or it can be less than this. The first one occurs when the fault has been extinguished after auto-reclosure and the second one occurs when the fault remains even after the auto-reclosure. The reason behind this difference is that fault point results in traveling waves reflection, and it can act like a remote terminal. This difference can be used to determine whether the fault still exists or it has been diminished. This can be written as:

$$\begin{aligned} \text{Successful Auto-reclosure : } \Delta_t &= 2 \times \frac{L}{v} \\ \text{Unsuccessful Auto-reclosure : } \Delta_t &< 2 \times \frac{L}{v} \end{aligned} \tag{5.6}$$

where, Δ_t is the time difference between the arrival time of the first and second traveling waves captured at the local terminal, l is the line length and v is the propagation velocity of traveling waves. Extensive simulations have been conducted to verify this scheme which are presented in the following section.

5.2 Simulation Results

The following sections provide some simulation results to prove the capacity of each of these criteria for use in after auto-reclosure cases. The simulation has been conducted on a 230kV power transmission line consisting of two power sources $S1$ and $S2$, three terminals (A , B and C), and one relay (R_B). Figure 24 presents the schematic of the simulation model where F is the fault modeling on this transmission line.

Table 9 shows the configuration of the simulated system, including the sequence and surge impedance of the transmission line.

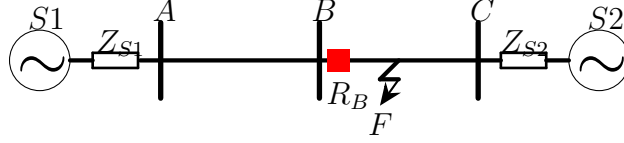


Figure 24: The 230-kV overhead line model

TABLE 9:
TRANSMISSION LINE ELECTRICAL PARAMETERS

Data	Source 1		Source 2	
	$ Z $ (ohm)	$\angle Z$ (deg)	$ Z $ (ohm)	$\angle Z$ (deg)
Positive Sequence	23.09	82.87	12.66	81.87
Zero Sequence	16.163	82.87	11.094	81.87

Overhead Transmission Line				
Data	R (pu)	X (pu)	B (pu)	Surge Imp. (pu)
Positive Sequence	0.0067	0.0957	0.1732	0.7432
Zero Sequence	0.0678	0.2495	0.1231	1.4234

5.2.1 Polarity of Traveling Waves after Auto-reclosure

Based on the theoretical background provided in Chapter Three and latter sections of this chapter, the presented criteria in use for normal condition of power system have been modified for the after auto-reclosure case. These criteria have been examined for different faults on the modeled power transmission line. However, the problem may arise for these logics due to traveling waves from the local and remote terminal coincide; but, in general practice of auto-reclosure there is enough time for the traveling wave induced by remote terminal breaker to damp before the local terminal breaker close. Additionally, the arrival time of these traveling waves at the local terminal is known and it can be easily distinguished from the traveling waves due to local breaker operation. The following sections will provide simulation results for each case provided in the proposed solution section of traveling waves polarity after auto-reclosure.

Current Traveling Waves after Auto-reclosure on Closed Power Line ($Z_L < Z_i$)

In this case, the remote terminal breaker has been closed; as a result, the line is energized. Table 10 provides the result of polarity analysis for different fault types, where Δ_{i1} and Δ_{i2} refer to the first and second current traveling waves captured at the local terminal. As Table 10 shows, in case of internal fault, at least the traveling wave on one phase shows a different polarity compared to the first traveling wave captured at the local terminal. However, as discussed, it cannot be used as the only criterion, as some fault types do not change the polarity of the reflected traveling wave; in other words, if the polarity of the traveling waves in one of the three phases change, there will be definitely fault on the power line; however, if the polarity of the current traveling waves on all phases remain the same, it does not mean there is no fault on the transmission line.

Current Traveling Waves after Auto-reclosure on Open Power Line

The same simulation can be carried out for power line with an open circuit at remote terminal, where the traveling waves as a result of the first breaker operation at local terminal will be utilized to determine whether the fault still exists or has been diminished after auto-reclosure. Table 11 provides the analysis on the polarity of traveling waves captured at local terminal, where in the case that at least the traveling wave on one phase showing the same polarity for the first and second traveling wave means that there is definitely fault on the transmission line after auto-reclosure. However, the opposite does not necessarily mean that there is no fault on the transmission line.

Voltage Traveling Waves after Auto-reclosure on Closed Power Line ($Z_L < Z_i$)

In this case, the voltage traveling waves has been considered. Although, it has drawbacks mentioned earlier due to difficulties in capturing, it provides an opportunity for another criterion to be used for single-ended protection after auto-reclosure. As a result, as Table 12 illustrates, extensive simulation has been conducted for different fault types where the power line is already closed from one end. As could be seen from (12), the traveling waves polarity will change due to the fault. As a result, in cases where fault still exists on the transmission line, the polarity of the traveling waves on at least one phase will change. However, as mentioned the opposite does not mean that there is no fault on the transmission line.

TABLE 10:
POLARITY OF CURRENT TRAVELING WAVES AFTER AUTO-RECLOSURE ON
CLOSED POWER LINE ($Z_L < Z_i$)

Fault type	TW order	Successful auto-reclosure			Unsuccessful auto-reclosure		
		A	B	C	A	B	C
AG	Δ_{i1}	+	-	-	-	-	-
	Δ_{i2}	+	-	-	+	-	-
BG	Δ_{i1}	+	-	-	-	-	-
	Δ_{i2}	+	-	-	+	-	+
CG	Δ_{i1}	+	-	-	+	+	+
	Δ_{i2}	+	-	-	-	-	+
ABG	Δ_{i1}	+	-	-	-	-	-
	Δ_{i2}	+	-	-	+	-	+
BCG	Δ_{i1}	+	-	-	+	-	+
	Δ_{i2}	+	-	-	+	-	+
ACG	Δ_{i1}	+	-	-	+	+	+
	Δ_{i2}	+	-	-	-	-	+
ABCG	Δ_{i1}	+	-	-	+	-	+
	Δ_{i2}	+	-	-	+	-	+
AB	Δ_{i1}	+	-	-	+	-	-
	Δ_{i2}	+	-	-	+	-	0
BC	Δ_{i1}	+	-	-	+	-	+
	Δ_{i2}	+	-	-	0	-	+
AC	Δ_{i1}	+	-	-	-	-	+
	Δ_{i2}	+	-	-	-	0	+
ABC	Δ_{i1}	+	-	-	+	-	+
	Δ_{i2}	+	-	-	+	-	+

Voltage Traveling Waves after Auto-reclosure on Open Power Line

The polarity of the voltage traveling waves as a result of the first breaker operation on open end power line have been investigated for different fault types in Table 13, where again Δ_{e1} and Δ_{e2} are the polarity of the first and second voltage traveling waves captured on each phases at local terminal. The first one is always the incident wave coming from the breaker, and the second one can be as a result of reflection from fault or remote terminal junction. As can be observed, the polarity of the traveling wave captured after successful

TABLE 11:
POLARITY OF CURRENT TRAVELING WAVES AFTER AUTO-RECLOSURE ON
OPEN POWER LINE ($Z_L > Z_i$)

Fault type	TW order	Successful auto-reclosure			Unsuccessful auto-reclosure		
		A	B	C	A	B	C
AG	Δ_{i1}	+	-	+	-	-	+
	Δ_{i2}	-	+	-	+	-	-
BG	Δ_{i1}	+	-	+	+	-	+
	Δ_{i2}	-	+	-	-	-	+
CG	Δ_{i1}	+	-	+	+	-	+
	Δ_{i2}	-	+	-	-	-	+
ABG	Δ_{i1}	+	-	+	-	-	+
	Δ_{i2}	-	+	-	+	-	+
BCG	Δ_{i1}	+	-	+	+	-	+
	Δ_{i2}	-	+	-	+	-	+
ACG	Δ_{i1}	+	-	+	-	-	+
	Δ_{i2}	-	+	-	-	-	+
ABCG	Δ_{i1}	+	-	+	+	-	+
	Δ_{i2}	-	+	-	+	-	+
AB	Δ_{i1}	+	-	+	+	-	+
	Δ_{i2}	-	+	-	+	-	0
BC	Δ_{i1}	+	-	+	+	-	+
	Δ_{i2}	-	+	-	0	-	+
AC	Δ_{i1}	+	-	+	+	-	+
	Δ_{i2}	-	+	-	-	0	+
ABC	Δ_{i1}	+	-	+	+	-	+
	Δ_{i2}	-	+	-	+	-	+

and unsuccessful auto-reclosure will be different compared to the incident wave. In the case of an internal fault, the traveling wave polarity will change at least on one phase versus the case of successful auto-reclosure where the fault has been diminished, and the polarity of traveling waves remains the same.

TABLE 12:
POLARITY OF VOLTAGE TRAVELING WAVES AFTER AUTO-RECLOSURE ON
CLOSED POWER LINE ($Z_L < Z_i$)

Fault type	TW order	Successful auto-reclosure			Unsuccessful auto-reclosure		
		A	B	C	A	B	C
AG	Δ_{e1}	+	-	-	-	-	-
	Δ_{e2}	-	+	+	-	+	+
BG	Δ_{e1}	+	-	-	-	-	-
	Δ_{e2}	-	+	+	-	+	-
CG	Δ_{e1}	+	-	-	+	+	+
	Δ_{e2}	-	+	+	+	+	-
ABG	Δ_{e1}	+	-	-	-	-	-
	Δ_{e2}	-	+	+	-	+	-
BCG	Δ_{e1}	+	-	-	+	-	+
	Δ_{e2}	-	+	+	-	+	-
ACG	Δ_{e1}	+	-	-	+	+	+
	Δ_{e2}	-	+	+	+	+	-
ABCG	Δ_{e1}	+	-	-	+	-	+
	Δ_{e2}	-	+	+	-	+	-
AB	Δ_{e1}	+	-	-	+	-	-
	Δ_{e2}	-	+	+	-	+	0
BC	Δ_{e1}	+	-	-	+	-	+
	Δ_{e2}	-	+	+	0	+	-
AC	Δ_{e1}	+	-	-	-	-	+
	Δ_{e2}	-	+	+	+	0	-
ABC	Δ_{e1}	+	-	-	+	-	+
	Δ_{e2}	-	+	+	-	+	-

5.2.2 Arrival Time of Traveling Waves after Auto-reclosure

The simulation study has been conducted to verify the traveling wave protection method based on its arrival time after auto-reclosure; however, before moving to simulation, it should be noted that the time needed for the traveling wave to be propagated from local terminal and returning after reflection from the remote terminal can be calculated using the following formula:

TABLE 13:
POLARITY OF CURRENT TRAVELING WAVES AFTER AUTO-RECLOSURE ON
OPEN POWER LINE ($Z_L > Z_i$)

Fault type	TW order	Successful auto-reclosure			Unsuccessful auto-reclosure		
		A	B	C	A	B	C
AG	Δ_{e1}	+	-	+	-	-	+
	Δ_{e2}	+	-	+	-	+	+
BG	Δ_{e1}	+	-	+	+	-	+
	Δ_{e2}	+	-	+	-	+	-
CG	Δ_{e1}	+	-	+	+	-	+
	Δ_{e2}	+	-	+	+	+	-
ABG	Δ_{e1}	+	-	+	-	-	+
	Δ_{e2}	+	-	+	-	+	-
BCG	Δ_{e1}	+	-	+	+	-	+
	Δ_{e2}	+	-	+	-	+	-
ACG	Δ_{e1}	+	-	+	-	-	+
	Δ_{e2}	+	-	+	+	+	-
ABCG	Δ_{e1}	+	-	+	+	-	+
	Δ_{e2}	+	-	+	-	+	-
AB	Δ_{e1}	+	-	+	+	-	+
	Δ_{e2}	+	-	+	-	+	0
BC	Δ_{e1}	+	-	+	+	-	+
	Δ_{e2}	+	-	+	0	+	-
AC	Δ_{e1}	+	-	+	+	-	+
	Δ_{e2}	+	-	+	+	0	-
ABC	Δ_{e1}	+	-	+	+	-	+
	Δ_{e2}	+	-	+	-	+	-

$$\Delta t = 2 \times \frac{l}{v} \quad (5.7)$$

where v indicates the propagation velocity and l is the line length. Considering the line length equal to $100km$ and the propagation velocity of $299670km/s$, the time needed by the traveling wave to reach remote terminal and return to the local terminal will be equal to 6.674×10^{-4} sec. Finally, adding it to the time of breaker operation will provide the arrival time for the traveling wave resulted by auto-reclosure and reflection by the remote

terminal equal to 0.5006674008 sec .

Figure 25 provides a simulation result for auto-reclosure on permanent AG fault located at 70 km away from local terminal as follows:

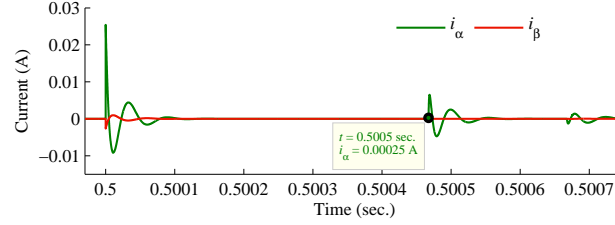


Figure 25: Current traveling waves of aerial modes after unsuccessful auto-reclosure for AG fault on overhead line

where the arrival time of the second traveling wave captured at the local terminal after unsuccessful auto-reclosure is:

$$t = 0.500467140825 \text{ sec.}$$

where, the time difference between the first and second traveling waves captured at local terminal (Δ_t) will be equal to 4.671×10^{-4} , which is less than the time needed for traveling wave to be propagated through the line, reflect by remote terminal and returning to the local terminal calculated by (5.7) as $6.674 \times 10^{-4} \text{ sec}$. This is because the fault still exists on the transmission line even after auto-reclosure. Figure 26 shows the same simulation; however, this time fault diminished after auto-reclosure.

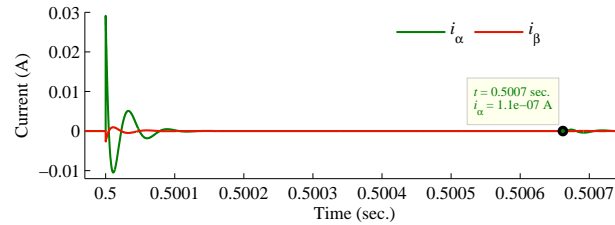


Figure 26: Current traveling waves of aerial modes after successful auto-reclosure for AG fault on overhead line

As Figure 26 shows, the arrival time of the second traveling wave after successful auto-reclosure is equal to $0.500667496444 \text{ sec.}$, which is the same as the time needed for traveling

wave to be propagated from the local terminal and returning with a reflection by the remote terminal. The same simulation can be conducted for *BG* fault, where Figure 27 provides the simulation for the traveling waves captured at local terminal after unsuccessful auto-reclosure.

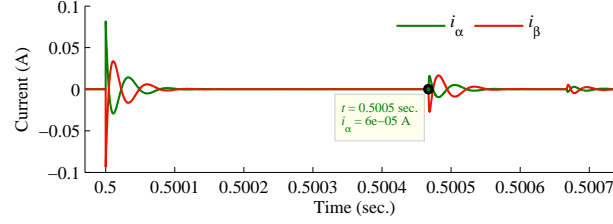


Figure 27: Current traveling waves of aerial modes after unsuccessful auto-reclosure for *BG* fault on overhead line

As can be seen, the arrival time of second traveling wave is 0.500466714083 and the time difference between the arrival time of first and second traveling wave (Δ_t) is equal to 4.667×10^{-4} , which is less than the time difference between successive traveling wave after successful auto-reclosure calculated as 6.674×10^{-4} . The same simulation can be conducted for successful auto-reclosure on *BG* fault too. As Figure 28 shows, the time difference between the arrival time of the first and second traveling waves is equal to 6.674×10^{-4} . It can be observed that this time is actually the same as the time difference for successive traveling waves after successful auto-reclosure on *AG* fault, as in both cases the fault is extinguished after the auto-reclosure.

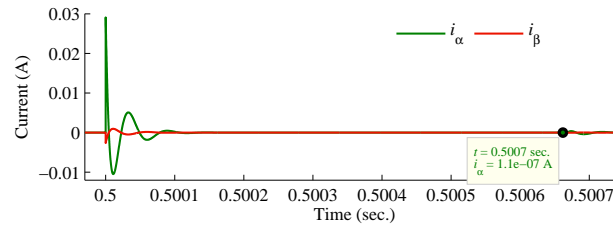


Figure 28: Current traveling waves of aerial modes after successful auto-reclosure for *BG* fault on overhead line

5.3 Conclusions

In this chapter, different protection schemes for after auto-reclosure protection have been presented, including the one based on polarity and arrival time of traveling waves. The method based on the arrival time of traveling waves can be used whether the transmission line is energized or not. However, the method based on the polarity of traveling waves will be more reliable for the case where the transmission line is open from one end. As in the case where transmission line is already closed from remote end, the polarity of the reflected traveling wave will depend on the characteristic impedance of the line and load impedance. Finally, considering all the mentioned methods and provided simulations, the proposed logics can be easily implemented to improve the security and reliability of the power system after auto-reclosure.

Chapter 6

Conclusions

6.1 Summary

The presented thesis considered different research topics, which all of them were finally connected to the main aim, namely the protection of transmission line after auto-reclosure using traveling waves. To reach it, PSCAD/EMTDC program and Matlab software were used to analyze traveling waves and verify the proposed schemes. In addition, different customized blocks were programmed to conduct simulations of which some are provided in Appendix A. The main topics discussed were the traveling waves attenuation by fault and propagation through transmission line as well as single-ended protection logics after auto-reclosure. For each of these topics, different schemes were proposed and simulated, and the effect of different factors was considered, which is provided as follows:

- For traveling waves attenuation as a result of fault and propagation through transmission line, this research included topics listed below.
 1. Traveling waves reflection and transmission after auto-reclosure: The theoretical background was provided and formed based on the research on this area and especially transmission line theory. It has been mentioned that fault results in traveling wave reflection and transmission, which its coefficient is based on the fault resistance and line impedance.
 2. Traveling waves reflection and transmission after auto-reclosure on hybrid lines: In hybrid lines which typically consist of overhead line and the small part of underground cables, there will be reflection and transmission of traveling waves

at the overhead line and underground cable intersection. The reflection and transmission coefficient will be directly affected by the characteristic impedance of the overhead line and underground cable. Its reflection and transmission coefficient is important as it affects the traveling wave attenuation after auto-reclosure.

3. Effect of fault resistance on traveling waves attenuation: In Chapter Four, the effect of fault resistance was considered for *AG* fault. Fault resistance of 0 to 100 Ω was examined, where it is shown that higher fault resistance results in higher attenuation. However, for external faults as the traveling waves originated by local breaker and captured at remote terminal do not pass through the fault, the attenuation of traveling wave will remain the same for different fault resistance.
 4. Effect of fault location on traveling waves attenuation: Fault location is another factor affecting traveling waves reflection and transmission coefficient, which is directly connected to its attenuation. It has been shown through extensive simulation that fault location has a negligible effect on the attenuation of the aerial components of traveling waves, which is also expected from the theory. This case has been considered for different fault types, where all results supported the theory.
 5. Effect of line length on traveling waves attenuation: It has been shown through extensive simulation, that increasing line length will increase traveling wave attenuation, whether there is or there is no fault on the transmission line. In addition, the rate of change for all those conditions remain the same. As a result, line length does not affect the proposed protection scheme.
 6. Attenuation in the energy of traveling waves: It has been mentioned that measuring traveling wave attenuation by the single sample is susceptible to noises; which is highly probable for real-life applications. As a result, this thesis first provided three sample criteria program, which can be found in appendix [A](#). Moreover, another method based on the attenuation in the energy of traveling waves has been suggested against the magnitude attenuation criterion. It has been shown that through different simulation, in some cases, it even work better than the method based on the attenuation in the magnitude of traveling waves and it is not also affected by any noise.
- For the single-ended traveling wave based protection algorithm after auto-reclosure, this thesis focused on the following subjects.
 1. The change in the polarity of traveling after auto-reclosure: The polarity of

successive traveling waves arriving at the local terminal has been analyzed for different fault types. Different protection schemes for voltage and current traveling waves have been provided. The case of open end (deadline) and the close end (live line) has been discussed, and protection schemes based on traveling waves polarity have been proposed for each of these cases. However, it is noted that the polarity of traveling waves can only be used as the supplementary scheme with other more secure methods.

2. The arrival time of traveling waves after auto-reclosure: It has been shown through theory and supported by simulation, that arrival time of second successive traveling wave at the local terminal will be directly affected by any kind of fault on the transmission line. In the case of permanent fault or unsuccessful auto-reclosure, the second traveling wave arrive at local terminal sooner than expected. The expected arrival time can be calculated based on line length and traveling waves propagation velocity and it can be employed to determine whether the fault still exists or it has been diminished after auto-reclosure.

6.2 Contributions

The contribution of this dissertation roughly falls on two subjects: analyzing the attenuation of traveling waves over its propagation through the power line, proposing double-ended traveling wave protection logic for after auto-reclosure and as well as proposing single-ended traveling wave based protection for after auto-reclosure.

6.2.1 Analysis on the Attenuation of Traveling Waves

Lack of reliable and high-speed power system protection schemes is still a problem for different industrial applications, particularly for Extra High Voltage (EHV). As a result, traveling wave methods were chosen for their super-fast operation. In this dissertation, traveling waves attenuation theory and simulation are provided and considered for power line protection after auto-reclosure. The presented double-ended traveling wave based protection after auto-reclosure can act as a new supplementary protection scheme, which can result in higher security and reliability for power systems.

6.2.2 Single-ended Traveling Wave Based Protection after Auto-reclosure

There are different reasons for considering the single-ended traveling wave based protection after auto-reclosure, as it mainly cost less to implement. The traveling wave based arrival time and polarity analysis elements are already installed in some commercial and industrial relays. Therefore, using them for protection after auto-reclosure will be extremely easy, and building the single-ended traveling wave based element for after auto-reclosure protection could be achieved using the existing hardware and equipment and there will be no extra cost for it.

6.3 Future Works

Further research on the traveling wave protection after auto-reclosure may include following topics:

1. Using other custom modal transform to improve the single-ended protection after auto-reclosure using the polarity of traveling waves,
2. Employing the proposed traveling wave attenuation based protection method for High Voltage Direct Current (HVDC) lines,

Bibliography

- [1] *Network Automation & Protection Guide, Protective Relays, Measurement & Control*, Alstom Grid, May 2011, pp. 233-247.
- [2] “Single phase tripping and auto reclosing of transmission lines-IEEE Committee Report,” in *IEEE Transactions on Power Delivery*, vol. 7, no. 1, pp. 182-192, Jan 1992.
- [3] Sang-Pil Ahn, Chul-Hwan Kim, R. K. Aggarwal and A. T. Johns, “An alternative approach to adaptive single pole auto-reclosing in high voltage transmission systems based on variable dead time control,” in *IEEE Transactions on Power Delivery*, vol. 16, no. 4, pp. 676-686, Oct 2001.
- [4] Yaozhong Ge, Fonghai Sui and Yuan Xiao, “Prediction methods for preventing single-phase reclosing on permanent fault,” in *IEEE Transactions on Power Delivery*, vol. 4, no. 1, pp. 114-121, Jan. 1989.
- [5] “IEEE Guide for Automatic Reclosing of Circuit Breakers for AC Distribution and Transmission Lines,” in *IEEE Std C37.104-2012 (Revision of IEEE Std C37.104-2002)*, vol., no., pp.1-72, July 6 2012
- [6] Jamali, Sadegh, and Navid Ghaffarzadeh. “Adaptive single-pole auto-reclosure for transmission lines using sound phases currents and wavelet packet transform.” *Electric Power Components and Systems* 38.14 (2010): 1558-1576.
- [7] A.P.Sakis Meliopoulos, *Power system grounding and transients*, Marcel Dekker, Inc, U.S.A, 1988.
- [8] H. W. Dommel, “Digital Computer Solution of Electromagnetic Transients in Single and Multiphase Networks”, *IEEE Transactions On Power Apparatus and Systems*, Vol.PAS-88, 4, April 1969, pp. 388 - 399.

- [9] J. P. Bickford, N. Mullineux, J. R. Reed, "Computation of power system transients", Stevenage 1976 , IEE monograph series.
- [10] F. V. Lopes, "Settings-Free Traveling-Wave-Based Earth Fault Location Using Un-synchronized Two-Terminal Data," in IEEE Transactions on Power Delivery, vol. 31, no. 5, pp. 2296-2298, Oct. 2016.
- [11] Phadke, Arun G., and James S. Thorp. Computer relaying for power systems. John Wiley & Sons, 2009.
- [12] Wei Chen, O. P. Malik, Xianggen Yin, Deshu Chen and Zhe Zhang, "Study of wavelet-based ultra high speed directional transmission line protection," in IEEE Transactions on Power Delivery, vol. 18, no. 4, pp. 1134-1139, Oct. 2003.
- [13] S. Marx, B. K. Johnson, A. Guzman , V. Skedzic, and M. V. Mynam, "Traveling Wave Fault Location in Protective Relays: Design, Testing, and Results." In proceedings of the 16th Annual Georgia Tech Fault and Disturbance Analysis Conference, Atlanta, GA, May 2013.
- [14] E. O. Schweitzer, III, A. Guzman, M. V. Mynam, V. Skedzic, B. Kasztenny, and S. Marx, "Locating Faults by the Traveling Waves They Launch," proceedings of the 40th Annual Western Protective Relay Conference, Spokane, WA, October 2013.
- [15] F. B. Costa, A. Monti, F. V. Lopes, K. M. Silva, P. Jamborsalamati and A. Sadu, "Two-Terminal Traveling-Wave-Based Transmission-Line Protection," in IEEE Transactions on Power Delivery, vol. 32, no. 3, pp. 1382-1393, June 2017.
- [16] F. Namdari and M. Salehi, "High-Speed Protection Scheme Based on Initial Current Traveling Wave for Transmission Lines Employing Mathematical Morphology," in IEEE Transactions on Power Delivery, vol. 32, no. 1, pp. 246-253, Feb. 2017.
- [17] A. Greenwood, Electrical Transients in Power Systems. New York: Wiley, 1991.
- [18] D. Wang, H.Gao,S. Luo and G. Zou, "Ultra-high-speed travelling wave protection of transmission line using polarity comparison principle based on empirical mode decomposition," Mathematical Problems in Engineering, 2015.
- [19] A. T. Johns and S. K. Salman, Digital Protection for Power Systems, ser. Inst. Elect. Eng. Power Eng. Series 15. London, U.K.: Peregrinus Ltd., 1995.

- [20] J. Wu, H. Li, G. Wang and Y. Liang, "An Improved Traveling-Wave Protection Scheme for LCC-HVDC Transmission Lines," in IEEE Transactions on Power Delivery, vol. 32, no. 1, pp. 106-116, Feb. 2017.
- [21] L. V. Bewley, *Traveling Waves on Transmission Systems*, Dover Publications Inc., New York, Second Edition, 1963.
- [22] D. E. Hedman, "Attenuation of Traveling Waves on Three-Phase Lines," in IEEE Transactions on Power Apparatus and Systems, vol. PAS-90, no. 3, pp. 1312-1320, May 1971.
- [23] G. L. Matthaei, L. Young, E. M. T. Jones, *Microwave Filters, Impedance-Matching Networks, and Coupling Structures*, McGraw-Hill, 1964.
- [24] L.A. Kojovic, J. Esztergalyos, "Traveling wave based relay protection," U.S. Patent 7 535 233, January 19, 2006.
- [25] C. C.Zhou, Q. Shu, and X. Y. Han, "A single phase earth fault location scheme for distribution feeder on the basis of the difference of zero mode traveling waves," *International Transactions on Electrical Energy Systems*, 27, no. 5, May 2017.
- [26] Aoyu Lei, X. Dong and S. Shi, "A novel method to identify the travelling wave reflected from the fault point or the remote-end bus," 2015 IEEE Power & Energy Society General Meeting, Denver, CO, 2015, pp. 1-5.
- [27] Marx, Stephen, Brian K. Johnson, Armando Guzmán, Veselin Skendzic, and Mangapathirao V. Mynam. "Traveling Wave Fault Location in Protective Relays: Design, Testing, and Results" In proceedings of the 16th Annual Georgia Tech Fault and Disturbance Analysis Conference, Atlanta, GA. 2013.

Appendices

Appendix A

PSCAD Customized Blocks for Traveling Waves

A.1 Traveling Wave First Zero Crossing Detection

This block will find the time of first zero cross of the traveling wave, which is helpful in analyzing traveling waves dispersion and attenuation due to transmission line characteristics.

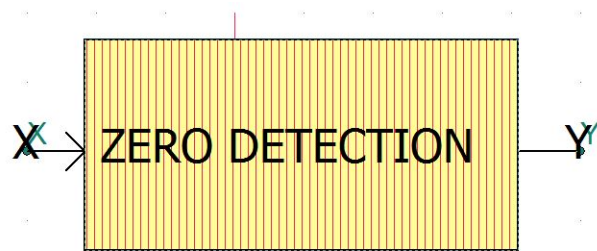


Figure 29: Customized traveling wave first zero cross detection block for PSCAD

```
#STORAGE REAL:2  
#LOCAL REAL X_OLD  
#LOCAL REAL Y_OLD  
X_OLD = STORF(NSTORF)
```

```

IF ((X_OLD<0 .and. $X>0) .or. ($X<0 .and. X_OLD>0)) $Y = TIME
STORF(NSTORF) = $X
NSTORF = NSTORF + 1

```

A.2 Three Point Signal Average

This block take average of three samples taken from traveling waves in order to reduce the analysis prone to system or instrument noises. The number of samples could be increased but it should be noted that the processing time will increase on the same hand.

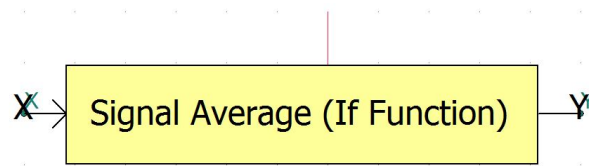


Figure 30: Customized three point signal average block for PSCAD

```

#STORAGE REAL:2
#LOCAL REAL A
#LOCAL REAL B
#LOCAL REAL C
#LOCAL REAL D
#LOCAL REAL X_OLD
#LOCAL REAL AVERAGE
#LOCAL INTEGER I
IF ($P==1) $Y = $X
IF ( $P.EQ.2 ) THEN
X_OLD = STORF(NSTORF)
A = X_OLD + $X
STORF(NSTORF) = $X
AVERAGE = A/2
$Y = AVERAGE
END IF
IF ( $P.EQ.3 ) THEN

```



```

X_OLD = STORF(NSTORF)
B = STORF(NSTORF + 1)
A = X_OLD + $X
C = B + $X
STORF(NSTORF) = $X
STORF(NSTORF + 1) = A
AVERAGE = C/3
$Y = AVERAGE
END IF
IF ( $P.EQ.4 ) THEN
X_OLD = STORF(NSTORF)
B = STORF(NSTORF + 1)
D = STORF(NSTORF + 2)
A = X_OLD + $X
C = B + $X
E = D + $X
STORF(NSTORF) = $X
STORF(NSTORF + 1) = A
STORF(NSTORF + 2) = C
AVERAGE = E/4
$Y = AVERAGE
END IF
IF ( $P.EQ.5 ) THEN
X_OLD = STORF(NSTORF)
B = STORF(NSTORF + 1)
D = STORF(NSTORF + 2)
F = STORF(NSTORF + 3)
A = X_OLD + $X
C = B + $X
E = D + $X
G = F + $X
STORF(NSTORF) = $X
STORF(NSTORF + 1) = A
STORF(NSTORF + 2) = C
STORF(NSTORF + 3) = E
AVERAGE = G/5
$Y = AVERAGE
END IF

```

$NSTORF = NSTORF + 4$

A.3 Integrator

This numerical integrator program could be used full in finding the area under the traveling waves and also its energy change through out its propagation.

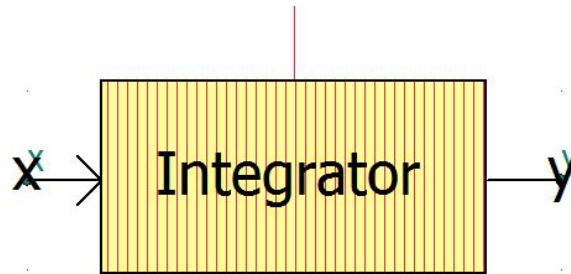


Figure 31: Customized integrator block

```
#STORAGE REAL:2
#LOCAL REAL X_OLD
#LOCAL REAL Y_OLD
MY_NSTORF = NSTORF
NSTORF = NSTORF + 2
X_OLD = STORF(MY_NSTORF)
Y_OLD = STORF(MY_NSTORF+1)
IF (TIMEZERO) Y_OLD=$Y0
$Y = Y_OLD + ($X + X_OLD)*0.5*DELT
STORF(MY_NSTORF) = $X
STORF(MY_NSTORF + 1) = $Y
```

A.4 Clark Transform

As there is no defined block for Clark transform in PSCAD software this block has been presented in order to be used for the modal analysis on traveling waves.

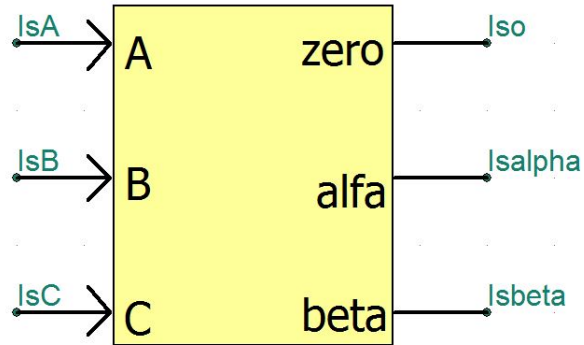


Figure 32: Clark transform block for PSCAD

```

$Isalpha = TWO_3RD*($IsA - $IsB*0.5 - $IsC*0.5)
$Isbeta = ($IsB - $IsC)*SQRT_1BY3
$Iso = ($IsA + $IsB + $IsC)/3

```

A.5 Peak Locator

This block illustrated in Figure 33, find the magnitude of the first traveling wave peak for traveling wave magnitude attenuation analysis.

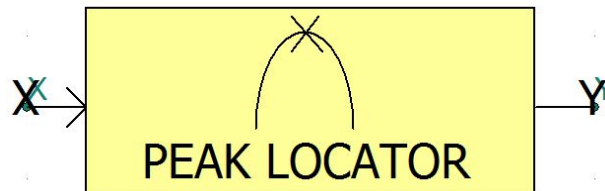


Figure 33: Traveling wave first peak detection

```

#STORAGE REAL:4
#LOCAL REAL X_OLD
#LOCAL REAL X_OLDER

```

```

#LOCAL REAL A
#LOCAL REAL C
X_OLD = STORF(NSTORF)
X_OLDER = STORF(NSTORF + 1)
A = X_OLD
C = X_OLDER
IF ($Y.GT.(0)) GOTO 11
IF ($X>0.1 .and. X_OLDER<X_OLD .and. X_OLD>$X) $Y = TIME
11 CONTINUE
STORF(NSTORF) = $X
STORF(NSTORF + 1) = A
NSTORF = NSTORF + 2

```

A.6 Traveling Waves Arrival Time Detection

This program is necessary to implement double-ended and single-ended fault location and fault protection methods, as most work on the arrival time. The necessary parameter for this block is the threshold value which should be chosen with great care to improve its accuracy.

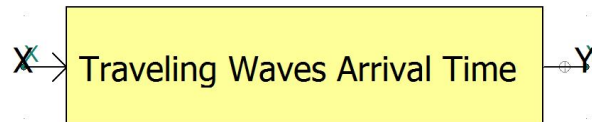


Figure 34: Traveling waves arrival time block for PSCAD

```

#STORAGE REAL:2
#LOCAL REAL X_OLD
#LOCAL REAL Y_OLD
X_OLD = STORF(NSTORF)
IF (STORF(NSTORF+1).GT.(0)) GOTO 7
IF ((ABS(X_OLD)<0.00004 .and. ABS($X)>0.00004) .or. (ABS($X)<0.00004 .and. -
-ABS(X_OLD)>0.00004)) STORF(NSTORF+1) = TIME
7 CONTINUE

```

```

STORF(NSTORF) = $X
$Y=STORF(NSTORF+1)
NSTORF = NSTORF + 2

```

A.7 Double-ended Traveling Wave Fault Location Relay

The double-ended traveling wave fault location relay has been implemented in PSCAD for the first time. The ability and accuracy of this block provide proof that all these methods could be implemented and used in real time simulation.

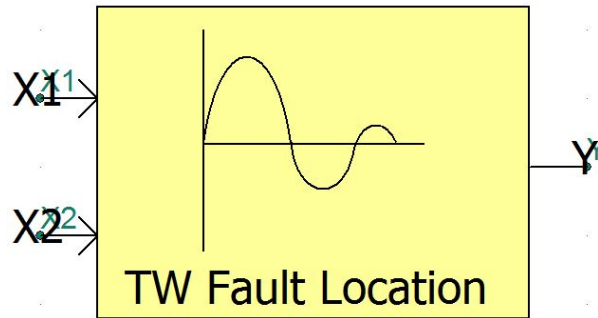


Figure 35: Double-ended traveling wave fault location relay designed in PSCAD

The set of input parameters necessary for this block are line length, traveling wave propagation velocity and setting point or the threshold value to capture arrival time. These parameters and input window could be seen in Figure 36 with sample data.

```

#STORAGE REAL:4
#LOCAL REAL X1_OLD
#LOCAL REAL Y1_OLD
#LOCAL REAL X2_OLD
#LOCAL REAL Y2_OLD
X1_OLD = STORF(NSTORF)
IF (STORF(NSTORF+1).GT.(0)) GOTO 9
IF ((ABS(X1_OLD)<$N .and. ABS($X1)>$N) .or. (ABS($X1)<$N .and.-

```

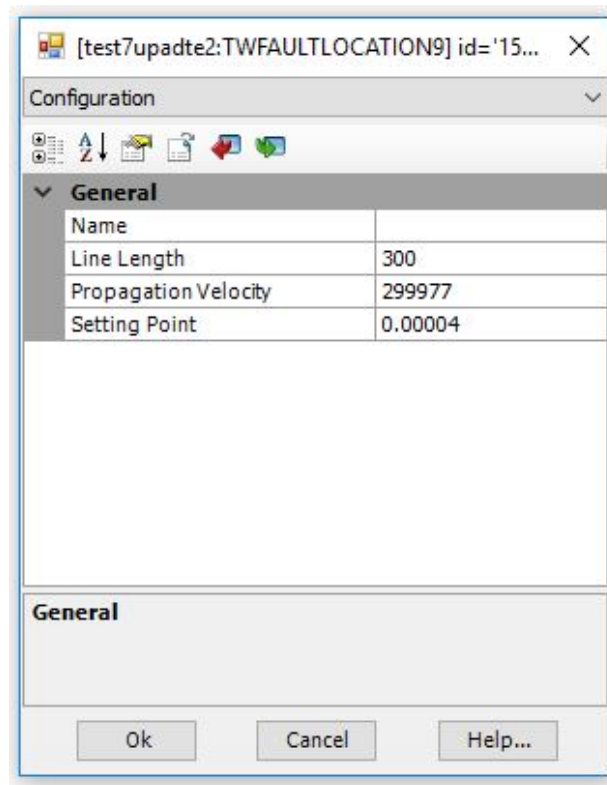


Figure 36: Defined parameters for double-ended traveling wave fault location relay

```

-ABS(X1_OLD)>$N)) STORF(NSTORF+1) = TIME
9 CONTINUE
STORF(NSTORF) = $X1
Y1=STORF(NSTORF+1)

X2_OLD = STORF(NSTORF+2)
IF (STORF(NSTORF+3).GT.(0)) GOTO 10
IF ((ABS(X2_OLD)<$N .and. ABS($X2)>$N) .or. (ABS($X2)<$N .and.-
-ABS(X2_OLD)>$N)) STORF(NSTORF+3) = TIME
10 CONTINUE
STORF(NSTORF+2) = $X2
Y2=STORF(NSTORF+3)

```

```
IF ((Y1.GT.(0)) .AND. (Y2.GT.(0))) $Y = 0.5*($L+(Y1-Y2)*$V)
NSTORF = NSTORF + 4
```